EUKARYOTIC CELL, June 2011, p. 803–819 Vol. 10, No. 6
1535-9778/11/$12.00 doi:10.1128/EC.00310-10

Calcineurin Controls Drug Tolerance, Hyphal Growth, and Virulence in *Candida dubliniensis*▽†

Ying-Lien Chen,[1] Alexandra Brand,[2] Emma L. Morrison,[2] Fitz Gerald S. Silao,[3] Ursela G. Bigol,[4] Fedelino F. Malbas, Jr.,[5] Jeniel E. Nett,[6,7,8] David R. Andes,[6,7,8] Norma V. Solis,[9] Scott G. Filler,[9,10] Anna Averette,[1] and Joseph Heitman[1]*

Department of Molecular Genetics and Microbiology, Duke University Medical Center, Durham, North Carolina[1]; Aberdeen Fungal Group, School of Medical Sciences, Institute of Medical Sciences, University of Aberdeen, Aberdeen, United Kingdom[2]; Department of Microbiology and Parasitology, University of Perpetual Help-Dr. Jose G. Tamayo Medical University, Biñan, Laguna, Philippines[3]; Environment and Biotechnology Division, Department of Science and Technology, Bicutan, Philippines[4]; Research Institute for Tropical Medicine, Alabang, Philippines[5]; Departments of Medicine[6] and Medical Microbiology and Immunology,[7] University of Wisconsin, and William S. Middleton Memorial Veterans Hospital,[8] Madison, Wisconsin; Los Angeles Biomedical Research Institute at Harbor-UCLA Medical Center, Torrance, California[9]; and David Geffen School of Medicine at UCLA, Los Angeles, California[10]

Received 9 December 2010/Accepted 11 April 2011

***Candida dubliniensis* is an emerging pathogenic yeast species closely related to *Candida albicans* and frequently found colonizing or infecting the oral cavities of HIV/AIDS patients. Drug resistance during *C. dubliniensis* infection is common and constitutes a significant therapeutic challenge. The calcineurin inhibitor FK506 exhibits synergistic fungicidal activity with azoles or echinocandins in the fungal pathogens *C. albicans*, *Cryptococcus neoformans*, and *Aspergillus fumigatus*. In this study, we show that calcineurin is required for cell wall integrity and wild-type tolerance of *C. dubliniensis* to azoles and echinocandins; hence, these drugs are candidates for combination therapy with calcineurin inhibitors. In contrast to *C. albicans*, in which the roles of calcineurin and Crz1 in hyphal growth are unclear, here we show that calcineurin and Crz1 play a clearly demonstrable role in hyphal growth in response to nutrient limitation in *C. dubliniensis*. We further demonstrate that thigmotropism is controlled by Crz1, but not calcineurin, in *C. dubliniensis*. Similar to *C. albicans*, *C. dubliniensis* calcineurin enhances survival in serum. *C. dubliniensis* calcineurin and *crz1*/*crz1* mutants exhibit attenuated virulence in a murine systemic infection model, likely attributable to defects in cell wall integrity, hyphal growth, and serum survival. Furthermore, we show that *C. dubliniensis* calcineurin mutants are unable to establish murine ocular infection or form biofilms in a rat denture model. That calcineurin is required for drug tolerance and virulence makes fungus-specific calcineurin inhibitors attractive candidates for combination therapy with azoles or echinocandins against emerging *C. dubliniensis* infections.**

Although *Candida albicans* is the most prevalent species causing candidiasis, >40% of *Candida* infections are now caused by evolutionarily diverged non-*albicans Candida* species (NACS). *Candida dubliniensis*, an emerging NACS that occurs globally, was first described as a separate species in 1995 (80), and its complete genome was recently sequenced (41). *C. dubliniensis* is the closest relative of the important human fungal pathogen *C. albicans* and commonly isolated from the oral cavities of patients with AIDS or individuals who are human immunodeficiency virus (HIV) positive and is occasionally found in the oral microflora of healthy individuals (78). Clinically, *C. dubliniensis* causes 2 to 7% of candidemia cases (40, 79), and it has been suggested that the gastrointestinal tract is a source of the *C. dubliniensis* in candidemia patients (13). Moreover, *C. dubliniensis* is now ranked as either the second or third most frequently isolated *Candida* species from patients with HIV/AIDS (6, 82). Interestingly, in addition to humans as the source, *C. dubliniensis* can be isolated from nonhuman sources, including ticks that parasitize seabirds (56) and the excrement of seabirds (49). Most avian *C. dubliniensis* isolates are genetically distinct from human isolates, but one avian isolate (AV7) has been shown to be indistinguishable from a human isolate by multilocus sequence typing (49), suggesting that transmission may occur between birds and humans.

C. dubliniensis isolates are susceptible to azole antifungal agents. However, *C. dubliniensis* can rapidly develop azole resistance during clinical therapy (52, 64). Chunchanur et al. recently reported that ~23% of *C. dubliniensis* isolates from HIV-infected patients were resistant to fluconazole (22). Moreover, *ERG11* mutations in *C. dubliniensis* isolated from HIV-infected individuals contribute to decreased susceptibility to fluconazole (64). Thus, new therapies that involve novel or combination drug treatments are needed. The calcineurin inhibitors tacrolimus (FK506) and cyclosporine A (CsA) target calcineurin through the intracellular receptor FK506 binding protein 12 (FKBP12) or cyclophilin A (CyA), respectively. Calcineurin is a eukaryotic calmodulin-dependent serine/threonine protein phosphatase. It forms a heterodimer protein consisting of the catalytic A (Cna1) and regulatory B (Cnb1) subunits, which are

* Corresponding author. Mailing address: Department of Molecular Genetics and Microbiology, Duke University Medical Center, Durham, NC 27710. Phone: (919) 684-2824. Fax: (919) 684-5458. E-mail: heitm001@duke.edu.

† Supplemental material for this article may be found at http://ec.asm.org/.

▽ Published ahead of print on 29 April 2011.

highly conserved between yeasts and mammals (3). In response to stress, the transcription factor Crz1 is dephosphorylated by calcineurin and then migrates to the nucleus to regulate expression of genes encoding cell wall biosynthetic enzymes and proteins involved in ion homeostasis (42, 72, 75, 76). Calcineurin is required for azole and/or echinocandin tolerance in *C. albicans* (61, 70, 84), *C. neoformans* (28, 45), and *A. fumigatus* (74); thus, the combination of a calcineurin inhibitor with either class of antifungal drug results in synergistic fungicidal activity.

The ability to undergo dimorphic transitions is integral to the virulence of *C. albicans*. The *C. albicans* ability to produce yeast cells is critical for dissemination, whereas the ability to form hyphae underlies survival and escape from macrophages and the ability to penetrate and invade tissues (15). Mutants locked in either the yeast (*cph1 efg1*) (47) or hyphal (*tup1*) form (14) exhibit attenuated virulence in murine systemic infection models. The role of the calcineurin pathway in hyphal growth of *C. albicans* is unclear. Two groups, including our own, found no role for calcineurin or Crz1 in hyphal growth (5, 62), while one group presented evidence interpreted to suggest a role for calcineurin and Crz1 in hyphal growth on filament-inducing media (42, 68). These differing results might be due to different genetic backgrounds of the strains or experimental protocols. *C. dubliniensis* is the only NACS capable of producing true hyphae, although morphogenesis is typically less robust than *C. albicans* on most filament-inducing media, which could explain its attenuated virulence in a murine systemic infection model compared with *C. albicans* (77). Thus, it is of interest to investigate the roles of calcineurin in hyphal growth and virulence in *C. dubliniensis*. In addition, *C. albicans* calcineurin and Crz1 are required for tropic responses, a phenotype linked to hyphal growth. *C. albicans* Crz1 is involved in thigmotropism and galvanotropism while calcineurin is involved in galvanotropism, suggesting that tropic responses are Crz1 dependent (9–11). In addition to hyphal growth, survival in serum is essential for pathogenic *Candida* species to disseminate and proliferate in the host. In *C. albicans*, calcineurin is required for serum survival (5, 8, 68). However, in the basidiomycete *C. neoformans*, calcineurin is not required for growth in serum and instead is required for growth at 37°C (59). Thus, fungal pathogens employ calcineurin in divergent roles to establish infection, while the mammalian host employs calcineurin as a defense against fungal infections via both innate immunity and adaptive immunity (37, 75).

In this study we investigate the roles of calcineurin in growth and pathogenesis in *C. dubliniensis*. We show that calcineurin is required for cell wall integrity, hyphal growth, serum survival, and virulence in *C. dubliniensis*, underscoring the importance of calcineurin as a global fungal virulence determinant and potential drug target. Furthermore, we demonstrate that calcineurin is required for azole or echinocandin tolerance, suggesting a possible combination therapy in *C. dubliniensis*, which frequently infects patients with HIV/AIDS.

MATERIALS AND METHODS

Yeast strains, media, and chemicals. Fungal strains used in this study are listed in Table 1. The following media were used in this study: YPD (1% yeast extract, 2% peptone, 2% glucose) liquid medium and agar (2%) plates, spider medium (10 g nutrient broth, 10 g mannitol, 4 g K_2HPO_4, 14 g Bacto agar in 1 liter double-distilled water [ddH_2O]; pH was adjusted to 7.2 with H_3PO_4), serum agar (50% serum, 2% agar), synthetic low-ammonium dextrose [SLAD; 1.7 g yeast nitrogen base without amino acids and without ammonium sulfate, 20 g glucose, 5 ml of 10 mM $(NH_4)_2SO_4$, 20 g Bacto agar in 1 liter of ddH_2O], and filament agar (FA; 1.7 g yeast nitrogen base without amino acids and without ammonium sulfate, 5 g glucose, 40 g Bacto agar in 1 liter ddH_2O). YPD medium containing 100 μg/ml nourseothricin was used to select transformants. The supplements FK506 (Astellas Pharma Inc.), cyclosporine A (CsA; LC Laboratories), sodium dodecyl sulfate (SDS; Fisher), fetal bovine serum (Invitrogen), calcofluor white (CFW; fluorescent brightener 28; Sigma), Congo red (Sigma), fluconazole (Bedford Laboratories), posaconazole (Sequoia Research Products Ltd.), voriconazole (Sigma), caspofungin (Merck), micafungin (Astellas Pharma Inc.), and anidulafungin (Pfizer Inc.) were added to the media at the concentrations indicated.

Strain construction. Both alleles of the *C. dubliniensis CNA1*, *CNB1*, and *CRZ1* genes were disrupted with the *SAT1* flipper (66). For the *CNA1* gene disruption, approximately 1-kb 5′ (amplified with primers JC57/JC58; see Table S1 in the supplemental material) and 3′ (amplified with primers JC59/JC60) noncoding regions (NCRs) of the *CNA1* open reading frame (ORF) were PCR amplified from genomic DNA of the wild-type strain CD36. The 4.2-kb *SAT1* flipper sequence was amplified from plasmid pSFS2A (66) with primers JC17/JC18. The three PCR products were treated with ExoSAP-IT (USB Corp.) to remove contaminating primers and deoxynucleotide triphosphates (dNTPs) and then combined in a 1:3:1 molar ratio (5′*CNA1*^{NCR}-*SAT1* flipper-3′*CNA1*^{NCR}) to generate the disruption allele by overlap PCR using flanking primers JC61/JC62 (~100 bp closer to the *CNA1* ORF compared with JC57/JC60, respectively, reserving primers JC57/JC60 for further integration confirmation), resulting in an ~6-kb 5′*CNA1*^{NCR}-*SAT1* flipper-3′*CNA1*^{NCR} *CNA1* disruption allele. The first allele of the *CNA1* gene was disrupted in the wild-type strain CD36 by transformation with 0.2 to 1 μg of gel-purified disruption DNA by electroporation (17). Two independent heterozygous nourseothricin-resistant mutants (YC31 and YC29; Table 1) were obtained from two separate transformations. Liquid YPM (1% yeast extract-2% peptone-2% maltose) medium was used to drive expression of the FLP recombinase under the control of *C. albicans MAL2* promoter (see Fig. S1 in the supplemental material). The *SAT1* flipper was then excised, leaving an FLP recombination target (FRT), and resulted in nourseothricin-sensitive *CNA1*/*cna1* mutant strains (YC36 and YC73). The second allele of the *CNA1* gene was disrupted with the same overlap PCR allele, resulting in nourseothricin-resistant homozygous *cna1*/*cna1* mutants YC40 and YC94 (Table 1). A similar approach was employed to disrupt the *CNB1* and *CRZ1* genes, with ~0.7-kb 5′ and 3′ noncoding regions for homologous recombination. To generate the ~5.4-kb *cnb1* disruption allele, the overlap PCR DNA products 5′*CNB1*^{NCR} (amplified with primers JC82/JC83), *SAT1* flipper (amplified with primers JC17/JC18), and 3′*CNB1*^{NCR} (amplified with primers JC86/JC87) were mixed in a 1:3:1 molar ratio and amplified with primers JC88/JC89 (~100 bp closer to the *CNB1* ORF compared with JC82/JC87, respectively). Two independent nourseothricin-resistant *cnb1*/*cnb1* mutants (YC87 and YC96; Table 1) derived from two separate transformations were obtained. To generate the ~5.4-kb *crz1* disruption allele, 5′*CRZ1*^{NCR} (amplified with primers JC100/JC101), *SAT1* flipper (amplified with primers JC17/JC18), and 3′*CRZ1*^{NCR} (amplified with primers JC102/JC103) were combined and amplified with primers JC104/JC105 (~100 bp closer to the *CRZ1* ORF compared with JC100/JC103, respectively). Two independent nourseothricin-resistant *crz1*/*crz1* mutants (YC107 and YC108; Table 1) derived from two separate transformations were obtained. These mutants were confirmed by PCR (data not shown) and validated by Southern blot analysis (Fig. S1).

The *CRZ1* complementation construct was made by amplifying a 0.45-kb fragment containing the 3′ NCR from CD36 genomic DNA with the JC320/JC321 primers that introduced SacII and SacI sites. This fragment was cleaved and ligated into the SacII-SacI-digested plasmid pGM175 (a gift from Gary Moran), resulting in pYC389. The 2.8-kb fragment containing the 5′ NCR and *CRZ1* ORF amplified with the JC288/JC289 primers that introduced KpnI and HindIII sites was cleaved and ligated into the KpnI-HindIII-digested pYC389, resulting in pYC393. The 8-kb fragment containing the *CRZ1* complementation allele and *SAT1* marker (see Fig. S2A in the supplemental material) was amplified from pYC393 with the JC288/JC321 primers, and this fragment was used to transform the nourseothricin-sensitive *crz1*/*crz1* mutant (YC280, derived from YC108; Table 1) to generate the *CRZ1*-complemented strain YC512 (Table 1). PCR and Southern blot analyses (Fig. S2A) were used to confirm the integration of the *CRZ1* complementation allele.

Southern blot analysis. Genomic DNA was isolated with the MasterPure yeast DNA purification kit (Epicentre Biotechnologies) from *C. dubliniensis* strains grown either in liquid YPD culture or on YPD plates. Twenty micrograms of

TABLE 1. *C. dubliniensis*, *C. albicans*, and *C. neoformans* strains used in this study

Strain	Genotype	Background	Reference
Candida dubliniensis			
CD36	Prototrophic wild type	Clinical isolate	80
YC31	*CNA1*/*cna1*::*SAT1-FLP*	CD36	This study
YC36	*CNA1*/*cna1*::*FRT*	YC31	This study
YC40[a]	*cna1*::*FRT*/*cna1*::*SAT1-FLP*	YC36	This study
YC29	*CNA1*/*cna1*::*SAT1-FLP*	CD36	This study
YC73	*CNA1*/*cna1*::*FRT*	YC29	This study
YC94[a]	*cna1*::*FRT*/*cna1*::*SAT1-FLP*	YC73	This study
YC47	*CNB1*/*cnb1*::*SAT1-FLP*	CD36	This study
YC69	*CNB1*/*cnb1*::*FRT*	YC47	This study
YC87[b]	*cnb1*::*FRT*/*cnb1*::*SAT1-FLP*	YC69	This study
YC41	*CNB1*/*cnb1*::*SAT1-FLP*	CD36	This study
YC82	*CNB1*/*cnb1*::*FRT*	YC41	This study
YC96[b]	*cnb1*::*FRT*/*cnb1*::*SAT1-FLP*	YC82	This study
YC81	*CRZ1*/*crz1*::*SAT1-FLP*	CD36	This study
YC102	*CRZ1*/*crz1*::*FRT*	YC81	This study
YC107[c]	*crz1*::*SAT1-FLP*/*crz1*::*SAT1-FLP*	YC102	This study
YC80	*CRZ1*/*crz1*::*SAT1-FLP*	CD36	This study
YC100	*CRZ1*/*crz1*::*FRT*	YC80	This study
YC108[c]	*crz1*::*FRT*/*crz1*::*SAT1-FLP*	YC100	This study
YC280	*crz1*::*FRT*/*crz1*::*FRT*	YC108	This study
YC512	*crz1*::*FRT*/*crz1*::*FRT* + *CRZ1*	YC280	This study
Candida albicans			
SC5314	Prototrophic wild type	Clinical isolate	36
SCCMP1M4	*cna1*::*FRT*/*cna1*::*FRT*	SC5314	5
SCCMP1MK2	*cna1*::*FRT*/*cna1*::*FRT* + *CNA1*	SCCMP1M4	5
DAY185	*ura3*/*ura3 his1*::*hisG*/*his1*::*hisG*::*HIS1* *arg4*::*hisG*/*arg4*::*hisG*::*ARG4*::*URA3*	BWP17	27
JRB64	*ura3*/*ura3 arg4*/*arg4 his1*/*his1 cnb1*::*URA3*/*cnb1*::*UAU1* + *HIS1*	BWP17	8
MCC85	*ura3*/*ura3 his1*::*hisG*::*CNB1-HIS1*/*his1*::*hisG* *arg4*::*hisG*/*arg4*::*hisG cnb1*::*UAU1*/*cnb1*::*URA3*	BWP17	26
OCC1.1	*ura3*/*ura3 his1*::*hisG*::*HIS1*/*his1*::*hisG arg4*::*hisG*/*arg4*::*hisG* *crz1*::*UAU1*/*crz1*::*URA3*	BWP17	62
OCC7	*ura3*/*ura3 his1*::*hisG*::*CRZ1-HIS1*/*his1*::*hisG* *arg4*::*hisG*/*arg4*::*hisG crz1*::*UAU1*/*crz1*::*URA3*	BWP17	62
CAF2-1	*ura3*/*URA3*	SC5314	32
DSY2091	*cna1*::*hisG*/*cna1*::*hisG*::*URA3*::*hisG*	CAF2-1	68
DSY2115	*cna1*::*hisG*/*cna1*::*hisG LEU2*::*CNA1*::*URA3*	CAF2-1	68
DSY2195	*crz1*::*hisG*/*crz1*::*hisG*::*URA3*::*hisG*	CAF2-1	42
MKY268	*crz1*::*hisG*/*crz1*::*hisG LEU2*::*CRZ1*/*URA3*	CAF2-1	42
Cryptococcus neoformans			
H99	Prototrophic wild type	Clinical isolate	65
KK1	*cna1*::*NAT*	H99	44

[a] Two independent *cna1*/*cna1* mutants.
[b] Two independent *cnb1*/*cnb1* mutants.
[c] Two independent *crz1*/*crz1* mutants.

DNA was subjected to Southern blot analysis. The genomic DNAs of the *cna1*/*cna1*, *cnb1*/*cnb1*, and *crz1*/*crz1* mutants were digested with PpuMI, HpaI, and EcoRV, respectively (see Fig. S1 in the supplemental material). PCR products containing 5′*CNA1*^{NCR} (amplified with primers JC57/JC58), 5′*CNB1*^{NCR} (amplified with primers JC82/JC83), and 3′*CRZ1*^{NCR} (amplified with primers JC102/JC103) were used as probes. Radiolabeled probes were generated using the Rediprime-it kit (Stratagene) and [α-^{32}P]dCTP (Easy Tides; Perkin-Elmer, Boston, MA). Ultrahyb buffer (Ambion) was used for prehybridization at 42°C, and hybridization and washing conditions were as described previously (17). Radioactive signals were exposed onto the storage phosphor cassette and digitalized with a Typhoon 9200 phosphorimager (Molecular Dynamics).

Spot growth assays. Cells were grown overnight at 30°C and washed twice with ddH_2O, and the optical density at 600 nm (OD_{600}) was measured. Cells were resuspended into an appropriate amount of ddH_2O to achieve 1 OD/ml. Three microliters of 5-fold serial dilutions (40 μl of 1-OD/ml cells plus 160 μl of ddH_2O as the first dilution in a 96-well plate) from each strain was spotted with a multichannel pipette onto solid media. The plates were then incubated at the indicated temperatures for 48 h and photographed.

Quantitative determination of expression by real-time reverse transcription-PCR (RT-PCR). Strains were grown overnight at 30°C and washed twice with ddH_2O. Cells were diluted to 0.2 OD/ml in YPD and incubated for 3 h at 30°C. Cells in log phase were then diluted to 0.2 OD/ml (10 ml) in YPD. Following 3 h of incubation at 30°C/250 rpm, cells were pelleted at 3,000 rpm at −4°C and stored at −80°C for further RNA extractions. The total RNAs were extracted using the RNeasy minikit (Qiagen). RNA purity and integrity were determined with a Nanodrop spectrophotometer and by gel electrophoresis, respectively. We used DNase I (Turbo DNA-free; Ambion) to eliminate genomic DNA contamination. Five hundred nanograms of DNA-free total RNAs was reverse transcribed to cDNA by the Affinity Script quantitative PCR (qPCR) cDNA synthesis kit (Agilent). PCR mixtures of 25 μl included 5 ng cDNA (in 10 μl), 12.5 μl of 2× qPCR master mix (Brilliant SYBR green kit; Agilent), 0.5 μl of 5 μM forward primer, 0.5 μl of 5 μM reverse primer, 1.125 μl of nuclease-free H_2O, and 0.375 μl of ROX dye. Quantitative PCR conditions were the following: 95°C for 10 min (denaturation); 95°C for 15 s and 60°C for 1 min (40 times, cycling stage); and 95°C for 15 s, 60°C for 1 min, and 95°C for 15 s (melting curve). Primers for probes were designed using Primer3 (http://frodo.wi.mit.edu/primer3/) and are

listed in Table S1 in the supplemental material. An ABI Prism 7900HT machine and StepOne software v2.1 (Applied Biosystems) were used to determine threshold cycle ($\Delta\Delta CT$) and relative quantity (RQ). The bar graphs of *ACT1*-normalized RQ compared with the wild type (CD36) were created with Prism 5.03.

Disk diffusion assays. Cells were grown overnight at 30°C and diluted to 1 OD/ml, and then 100 μl (0.1 OD) was spread onto YPD in the absence or presence of FK506 (1 μg/ml) or CsA (100 μg/ml). After 10 min, sterile disks were placed onto the surface of the agar. Ten microliters of 0.1-μg/μl fluconazole (1 μg total) or H_2O (control) was spotted onto the sterile disk after placement on the medium. The plates were then incubated at 30°C for 24 h and photographed.

Time-kill curve for strains exposed to fluconazole. Cells were grown overnight at 30°C and washed twice with ddH_2O. Cells were separated by sonication (Branson sonicator 250) at a constant of 2 for 10 s and counted with a hemocytometer. Cells (5×10^6) were added to 5 ml of fresh YPD medium to achieve 10^6 cells/ml in the absence or presence of fluconazole (10 μg/ml). Cells were cultured at 30°C with shaking at 250 rpm. The cells surviving after 0, 3, 6, 9, and 24 h were serially diluted onto YPD medium, and CFU were counted after 48 h of incubation. The experiments were performed in triplicate, and data were plotted using Prism 5.03.

Germ tube formation assays. Cells were grown overnight and washed twice with ddH_2O. Cells were diluted to 1 OD/ml and sonicated to separate slightly clumped cells. Two microliters of cells was added to microtiter wells prefilled with 98 μl of serum or spider medium, resulting in 0.002 OD ($\sim 4 \times 10^4$ cells) in each well. Strains were confirmed to have no germ tubes at 0 h and were incubated at 37°C for the indicated times. The percentage of germ tube formation was counted using the following formula [(germ tube cells)/(germ tube + yeast cells)] × 100%. At least 200 cells were counted in each experiment of three independent experiments.

Thigmotropism assays. Poly-L-lysine-coated quartz slides featuring ridges of 0.79 μm ± 40 nm and a pitch of 25 μm (Kelvin Nanotechnology, Glasgow, United Kingdom) (11) were prepared by treatment with UV-ozone for 2 min followed by coating with 0.01% (wt/vol) poly-L-lysine (150,000 to 333,000 M_w; Sigma, United Kingdom) for 30 min. Slides were rinsed with ddH_2O and left overnight to dry in a sterile petri dish. Yeast cells were grown overnight in 5 ml YPD with shaking at 200 rpm. A volume of 7.5 μl was added to 10 ml ddH_2O. After vortexing, the suspension was poured over a quartz slide and cells were allowed to adhere at room temperature for 30 min. Slides were lightly rinsed with ddH_2O to remove unadhered cells and placed in 20 ml prewarmed 20% (vol/vol) newborn calf serum containing 2% (wt/vol) glucose at 37°C for 6 h to induce hyphae. The number of hyphae reorienting on contact with a ridge was determined by light microscopy, and tip reorientations were expressed as a percentage of the total observed interactions. At least 100 interactions were observed per strain in each experiment, and results were reported as the mean value from three independent experiments ± standard deviation (SD).

Murine systemic infection model. Five- to 6-week-old male CD1 mice from Jackson Laboratories ($n = 15$ for each group, except $n = 10$ for *C. albicans*) were used in this study. *C. dubliniensis* and *C. albicans* strains were grown in 5 ml YPD overnight at 30°C with shaking at 250 rpm. Cultures were washed twice with 10 ml of phosphate-buffered saline (PBS), and the cells were then resuspended in 2 ml of PBS. Modestly clumped cells were dispersed by sonication. Cells were counted with a hemocytometer and resuspended in an appropriate amount of PBS to obtain an infection inoculum of 2.5×10^7 cells/ml. Two hundred microliters (5×10^6 cells) was used to infect mice by lateral tail vein injection. The course of infection was monitored for up to 42 days. The survival of mice was monitored twice daily, and moribund mice (unable to eat or drink, body weight reduced by >30%, severely tilted head, or hunched) were euthanized with CO_2. All experimental procedures were carried out according to NIH guidelines and Duke University Institutional Animal Care and Use Committee (IACUC) protocols for the ethical treatment of animals. Appropriate dilutions of the cells were plated onto YPD and incubated at 30°C for 48 h to confirm cell viability.

To determine fungal burden, the left kidney of *C. dubliniensis*-infected mice ($n = 5$ for each strain, except $n = 4$ for strain YC107 due to a death immediately following injection) was dissected at day 7. The organs were weighed, transferred to a 15-ml Falcon tube filled with 5 ml PBS, and homogenized for 10 s at 19,000 rpm/min (IKA T25; Cole-Parmer). Tissue homogenates were serially diluted, and 100 μl was plated onto a YPD plate. The plates were incubated at 30°C for 48 h to determine CFU per gram of kidney. The identity of organ-recovered colonies was confirmed by PCR and by growth or no growth on YPD medium containing 0.01% SDS. For histopathological analysis, kidneys were excised at day 14, fixed in 10% phosphate-buffered formalin (Fisher), and Gomori methenamine silver (GMS) and hematoxylin and eosin (H&E) stainings were performed by the Department of Pathology at Duke University. After slide preparation, each sample was examined thoroughly by microscopy for analysis of *Candida* colonization (GMS) and tissue necrosis (H&E). Images were captured using an Olympus Vanox microscope (PhotoPath; Duke University Medical Center).

Murine ocular infection model. Cells were grown in YPD broth overnight at 37°C. Cultures were pelleted by centrifugation (10,000 rpm for 15 min) and washed three times with sterile PBS (pH 7.4). Cells were suspended and diluted in sterile PBS to yield a fungal concentration of 10^6 cells/5 μl. Concentration was determined by using spectrophotometer optical density reading at a 600-nm wavelength and multiplying it with a conversion factor of 1 OD_{600}, equivalent to 3×10^7 cells/ml. Inoculum concentration was verified by plating on YPD for 48 h at 37°C.

For murine ocular infection, outbred ICR mice (Research Institute for Tropical Medicine, Alabang, Philippines) around 6 to 8 weeks of age (20 to 25 g) were used in the experiment in accordance with the ARVO statement for the Use of Animals in Ophthalmic and Vision Research. An experimental keratomycosis protocol described previously (89) was used for *C. dubliniensis* with minor modifications and was approved by the University of Perpetual Help Institutional Review Board. Mice were maintained in comfortable cages with a constant supply of food and water, and the cages were periodically sanitized with Sterilium to minimize potential other infections during the course of the observations. Mice were immunocompromised by intraperitoneal injection of cyclophosphamide (180 to 200 mg/kg body weight; Sigma-Aldrich) predissolved in sterile 0.9% NaCl 5 days, 3 days, and 1 day before the inoculation. Prior to inoculation, mice were anesthetized by intramuscular injection of Zoletil 50 (15 mg/kg body weight; Virac, Australia) followed by topical application of proparacaine hydrochloride ophthalmic solution (Alcaine; Alcon-Couvreur, Belgium) to the eyes. Once animals were anesthetized, the right eye was superficially scarified in a grid pattern with a sterile 25-gauge hypodermic needle. Five microliters of *Candida* solution (10^6 cells) was placed into each eye. Inoculum was distributed uniformly by rubbing the eye with the eyelid. A mock-infection experiment was performed using sterile PBS as control. Disease severity of fungal keratitis was assessed for 8 days with the aid of a dissecting microscope based on the procedure described previously (89). In this procedure, corneal involvement was assessed and scored according to three parameters, namely, (i) area of opacity, (ii) density of opacity, and (iii) surface regularity. A grade of 0 to 4 was assigned on each of these criteria to yield a maximum score of 12.

Wax moth infection studies. Wax moths (*Galleria mellonella*) of the final-instar larval stage (~0.3 g) from Vanderhorst (Ohio) were used (10 per strain) within 7 days from the day of shipment. The larval infection protocol was adapted from previously described methods for *C. neoformans* (53) with minor modifications. Each larva was infected with 10^6 *C. dubliniensis* or *C. albicans* cells in 5 μl PBS by injection into the last pseudopod and incubated at 24°C in a petri dish with wood shavings. Larvae showing signs of severe morbidity, such as change of body color and no response to touch, were sacrificed by cold treatment at −20°C. The number of surviving wax moths was monitored and recorded daily.

Epithelial cell interactions. The extent of damage to oral epithelial cells caused by *C. dubliniensis* compared to *C. albicans* was determined by a minor modification of our previous method (63). Briefly, the FaDu oral epithelial cell line (American Type Culture Collection) was grown to 95% confluence in a 24-well tissue culture plate and loaded with ^{51}Cr overnight. The following day, the cells were rinsed extensively to remove the unincorporated tracer. Next, they were infected with either 2×10^8 yeast cells of *C. dubliniensis* CD36 or 5×10^5 yeast cells of *C. albicans* SC5314 in 1 ml of RPMI 1640 medium. After 2, 4, and 6 h, an aliquot of the medium above the cells was withdrawn for determination of ^{51}Cr content. Control wells containing uninfected epithelial cells were processed in parallel to determine the spontaneous release of ^{51}Cr. At the end of the experiment, the cells were lysed with NaOH and the wells were rinsed with RadiacWash (Atomic Products). The lysate and rinses were collected, and their ^{51}Cr content was determined. Each organism was tested in triplicate wells.

Differential interference contrast microscopy was used to examine the morphology of the organisms when they were in contact with epithelial cells. FaDu oral epithelial cells were grown to 95% confluence on fibronectin-coated glass coverslips (12-mm diameter) in 24-well tissue culture plates. The epithelial cells were infected with either 10^5 cells of *C. dubliniensis* CD36 or 5×10^4 cells of *C. albicans* SC5314 in 1 ml of RPMI 1640 medium for 2, 4, or 6 h. Next, the coverslips were rinsed once with PBS and then fixed for 15 min with 3% paraformaldehyde in PBS. They were then rinsed in PBS, mounted inverted on microscope slides, and imaged by confocal microscopy.

Rat denture biofilm model. Denture appliances were placed in specific-pathogen-free male Sprague-Dawley rats weighing ~350 g (Harlan Sprague-Dawley, Indianapolis, IN) as previously described (54). Animals were anesthetized and immunosuppressed with a single dose of cortisone (200 mg/kg subcutaneously [SQ]) on the day of infection and received ampicillin-sulbactam, 100 mg/kg twice

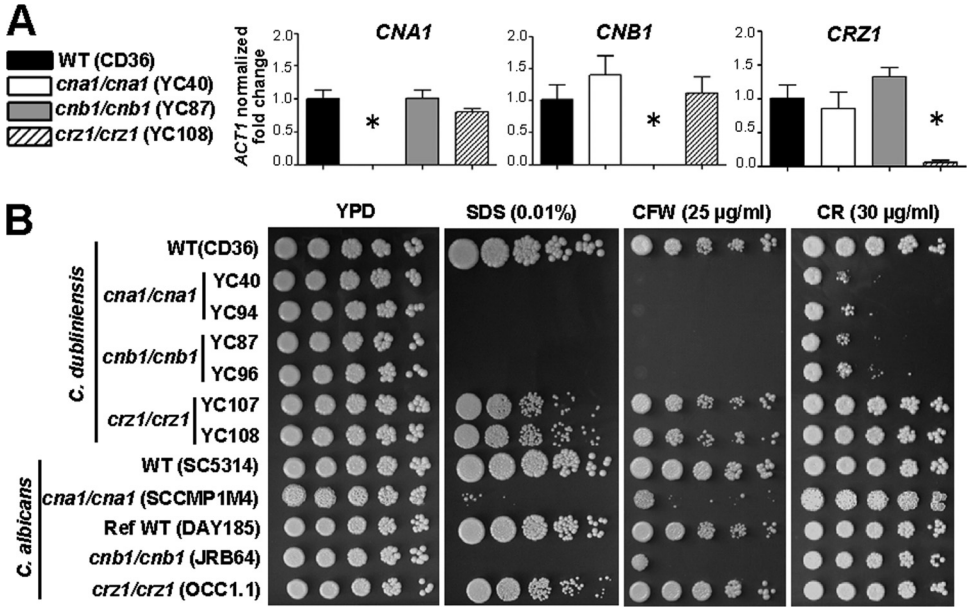

FIG. 1. Calcineurin mutations result in defective cell wall integrity in *C. dubliniensis*. (A) Expression of the calcineurin and *CRZ1* genes in the wild-type and mutant strains was quantified by real-time PCR. The fold changes in transcription of *CNA1*, *CNB1*, and *CRZ1* were normalized to the endogenous control *ACT1*. The data are represented as means ± SDs of triplicate measurements. One representative graph is shown from three independent experiments. Asterisks indicate $P < 0.0001$ compared with the wild type. (B) Cells were grown overnight in YPD at 30°C, 5-fold serially diluted, and spotted onto YPD medium containing sodium dodecyl sulfate (SDS), calcofluor white (CFW), or Congo red (CR) and incubated at 30°C for 48 h. WT, wild type.

a day (BID), during the course of the experiment. A 32-gauge stainless steel Babcock orthodontic wire (Miltex) was threaded across the hard palate and secured between cheek teeth (54). Teeth were etched with Uni-Etch 32% semigel etchant with benzalkonium chloride (Bisco, Inc.). A metal spatula was placed over the hard palate to create a space for *Candida* inoculation. Cold cure acrylic temporary crown and bridge material (HP MaxiTemp; Henry Schein) was applied over cheek teeth and wire and was allowed to solidify for 5 min. After removal of the spatula, the hard palate beneath the acrylic device was inoculated with *Candida* at 10^8 cells/ml (0.1 ml). Animals were sacrificed after 48 h of denture placement, and devices were processed for scanning electron microscopy (SEM) as previously described (2, 54). Briefly, devices were washed with PBS and placed in fixative (1% [vol/vol] glutaraldehyde and 4% [vol/vol] formaldehyde in PBS) overnight. The samples were rinsed with PBS, treated in 1% osmium tetroxide for 30 min, and rinsed with PBS. The samples were then dehydrated in a series of ethanol washes, and final desiccation was accomplished by critical-point drying (Tousimis, Rockville, MD). Specimens were mounted on aluminum stubs and sputter coated with gold. Dentures were imaged on a JEOL 6100 at 10 kV. The images were processed for display using Adobe Photoshop.

Animals were maintained in accordance with the American Association for Accreditation of Laboratory Animal Care (AAALAC) criteria, and all studies were approved by the Institutional Animal Care and Use Committee (IACUC).

Statistical analysis. Statistical analysis was conducted using Prism 5.03 software (GraphPad, La Jolla, CA), with the exception that SPSS software was used to analyze thigmotropic responses (Dunnett's *t* test). For the mouse and *Galleria* larval infection studies, Kaplan-Meier survival curves were generated and the log-rank (Mantel-Cox) test was employed to compare significance. The significance of differences in fungal burden, germ tube formation, and real-time RT-PCR was determined using one-way analysis of variance (ANOVA) and Dunnett's multiple comparison tests. The significance of the capacity of *Candida* species to cause damage to oral epithelial cells and murine corneas was determined by unpaired *t* test and Student's *t* test, respectively. A *P* value of <0.05 was considered significant.

RESULTS

Calcineurin mutation confers cell wall integrity defects in *C. dubliniensis*. The newest class of antifungal drugs in clinical use, the echinocandins, target fungal cell wall synthesis. Therefore, there is increased interest in the study of *Candida* cell wall integrity (19, 26, 87). Recently, Jackson et al. reported that the genome sequences of *C. dubliniensis* and *C. albicans* are highly conserved with considerable synteny, with the exception of 168 species-specific genes which included cell wall-related secreted aspartyl protease and agglutinin-like protein families (41). Calcineurin is required for cell wall integrity in *C. albicans* (26, 68) and *A. fumigatus* (73), but it is not known if calcineurin has an analogous role in *C. dubliniensis*. The *C. dubliniensis* orthologs of *C. albicans CNA1*/*CMP1* and *CNB1* and the calcineurin target *CRZ1* genes were identified by reciprocal BLAST searches between the two species and in all cases identified a reciprocal best BLAST hit ortholog as the *C. dubliniensis CNA1* (CD36_00650), *CNB1* (CD36_54760), and *CRZ1* (CD36_85720) genes. *C. dubliniensis* Cna1, Cnb1, and Crz1 share 91%, 100%, and 81% identity, respectively, over the full-length proteins with their corresponding *C. albicans* orthologs. Calcineurin A (Cna1) has the conserved calcineurin B binding, calmodulin-binding, and autoinhibitory regions. Calcineurin B (Cnb1) has four EF-hand Ca^{2+} binding motifs, while Crz1 shares zinc finger domains with the respective ortholog in *C. albicans*. Two independent calcineurin and *crz1*/*crz1* mutants were generated using the *SAT1* flipper cassette and confirmed by PCR and Southern blot analysis. Real-time RT-PCR analysis confirmed loss of expression of the *CNA1*, *CNB1*, or *CRZ1* gene in the respective null mutant strains (Fig. 1A).

The cell wall integrity of the *C. dubliniensis* calcineurin (*cna1*/*cna1* and *cnb1*/*cnb1*) and *crz1*/*crz1* mutants was assayed by growing them in the presence of SDS, a reagent which compromises cell membrane/wall integrity; calcofluor white (CFW), which destabilizes chitin polymerization; and Congo

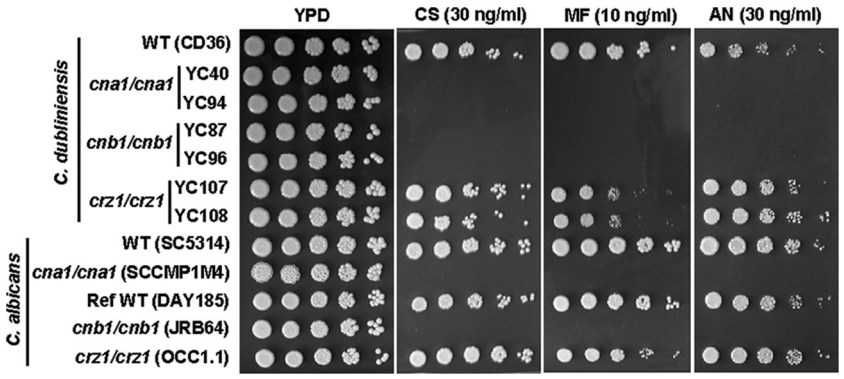

FIG. 2. Calcineurin mutations enhance fungicidal activity of echinocandins in *C. dubliniensis*. Cells were grown overnight in YPD at 30°C, 5-fold serially diluted, and spotted onto YPD medium containing caspofungin (CS), micafungin (MF), or anidulafungin (AN) at the concentrations indicated. The plates were incubated at 30°C for 48 h and photographed.

red, which intercalates between glucan polymers (30, 67, 83). Similarly to *C. albicans* (26, 42, 62, 68), *C. dubliniensis* calcineurin mutants exhibited hypersensitivity to SDS, while *crz1*/*crz1* mutants exhibited a phenotype intermediate between the wild type and calcineurin mutants (Fig. 1B), suggesting that cell membrane/wall integrity controlled by calcineurin is at least in part Crz1 dependent in *C. dubliniensis*. The slower growth of these mutants on YPD medium containing SDS compared with the wild type was not attributable to defects in thermal stress tolerance (see Fig. S3A in the supplemental material) or growth rate (Fig. S3B).

C. dubliniensis calcineurin, but not *crz1*/*crz1*, mutants were hypersensitive to CFW (Fig. 1B), suggesting an essential role of calcineurin in cell wall integrity. Interestingly, *C. dubliniensis* calcineurin mutants were hypersensitive to Congo red, while *C. albicans* calcineurin mutants exhibited wild-type growth (Fig. 1B; up to 50 μg/ml). This indicates that calcineurin plays a greater role in cell wall integrity in *C. dubliniensis* than in *C. albicans*. To examine if hypersensitivity to CFW and Congo red of the *C. dubliniensis* calcineurin mutants was due to affected chitin synthesis, we exposed the cells to nikkomycin Z, a chitin synthase inhibitor (90). None of the mutants in either species was hypersensitive to nikkomycin Z (1 to 10 μg/ml) (data not shown), in contrast to a calcineurin mutant (*cnaA*) of *A. fumigatus* (33). This suggests a distinct role of calcineurin governing chitin synthesis in *Candida* and *Aspergillus*.

***C. dubliniensis* calcineurin mutants exhibit echinocandin hypersusceptibility.** Echinocandins (caspofungin, micafungin, and anidulafungin) are a new class of antifungal drugs that noncompetitively inhibit the cell wall biosynthetic enzyme β-1,3-glucan synthase, an essential enzyme in fungal pathogens. Kofteridis et al. recently reported that ~1% (7/650) of *Candida* isolates from cancer patients with candidiasis are caspofungin resistant (43). Resistance has also been reported in other *Candida* clinical isolates (86), suggesting a need for alternative therapy for invasive fungal infections. Singh et al. demonstrated that calcineurin inhibitors (FK506 and CsA) exhibit fungicidal activity with micafungin (at a nonfungicidal concentration) against *C. albicans* (70), indicative of a potential combination therapy. However, synergism between calcineurin inhibitors and echinocandins has not yet been investigated in *C. dubliniensis*.

Here, we report that, similar to *C. albicans* calcineurin mutants, *C. dubliniensis cna1*/*cna1* and *cnb1*/*cnb1* mutants are hypersusceptible to caspofungin, micafungin, and anidulafungin compared with the wild type (Fig. 2). Interestingly, *C. dubliniensis crz1*/*crz1* mutants exhibited differential responses to echinocandins. *C. dubliniensis crz1*/*crz1* mutants showed an intermediate hypersusceptibility to micafungin compared with the wild type and calcineurin mutants, suggesting that micafungin tolerance is mediated by Crz1. However, caspofungin and anidulafungin did not affect the growth of *crz1*/*crz1* mutants (Fig. 2). To test if calcineurin is required for resistance to caspofungin, we determined the MIC for the *C. dubliniensis* calcineurin and *crz1*/*crz1* mutants using Etest concentration-gradient diffusion assays. The MIC for *C. dubliniensis cna1*/*cna1* and *cnb1*/*cnb1* mutants was 0.016 μg/ml (clear inhibition zone) compared with 0.064 μg/ml (turbid inhibition zone) for the wild type, suggesting that calcineurin plays a role in caspofungin resistance in *C. dubliniensis* (Table 2). The MIC for the *C. dubliniensis crz1*/*crz1* mutant (0.094 μg/ml) was not significantly different from the wild type (Table 2). As a control experiment, FK506 decreased caspofungin resistance in both the wild type and the *crz1*/*crz1* mutant but not in the calcineurin mutants (Table 2), confirming that resistance to caspofungin in *C. dubliniensis* is orchestrated by calcineurin signaling.

Fluconazole tolerance is governed by calcineurin and Crz1 in *C. dubliniensis*. Azole-resistant *C. dubliniensis* is frequently isolated from the oral cavities of HIV/AIDS patients (6, 82). A calcineurin inhibitor and fluconazole exhibited synergistic fungicidal activity against *C. albicans* (26) and *C. neoformans* (28). To test our hypothesis that calcineurin is required for fluconazole tolerance in *C. dubliniensis*, we used spot, disk diffusion, and time-killing curve assays. *C. dubliniensis cna1*/*cna1* and *cnb1*/*cnb1* mutants were hypersusceptible to fluconazole while *crz1*/*crz1* mutants exhibited susceptibility intermediate between the wild type and the calcineurin mutants (Fig. 3A), suggesting that other regulators control fluconazole tolerance in addition to Crz1. This is similar to *C. albicans* calcineurin and *crz1*/*crz1* mutants, suggesting that azole tolerance governed by the calcineurin pathway has been conserved during evolution of the two *Candida* species. By disk diffusion assays, we found that pharmacological inhibition of calcineurin phenocopies calcineurin deletion while *crz1*/*crz1* mutants exhibit an interme-

TABLE 2. Calcineurin is required for caspofungin resistance in *C. dubliniensis*[a]

Strain	No FK506		FK506 (1 μg/ml)	
	Caspofungin (MIC or range; μg/ml)	Inhibition zone	Caspofungin (MIC or range; μg/ml)	Inhibition zone
CD36 (wild type)	0.064	Turbid	0.016	Clear
cna1/*cna1* (YC40)	0.016	Clear	0.016	Clear
cna1/*cna1* (YC94)	0.016	Clear	0.012–0.016	Clear
cnb1/*cnb1* (YC87)	0.016	Clear	0.016–0.023	Clear
cnb1/*cnb1* (YC96)	0.016	Clear	0.016	Clear
crz1/*crz1* (YC107)	0.094	Turbid	0.016	Clear
crz1/*crz1* (YC108)	0.094	Turbid	0.016–0.023	Clear

[a] Cells were grown overnight at 30°C and washed twice with ddH_2O. Then 0.5 OD (in 500 μl) of cells was spread on RPMI 1640 medium (Remel; R04067) in the absence or presence of FK506 (1 μg/ml). After 10 min, the Etest caspofungin strip (bioMérieux Corp.) was transferred to the surface of the medium. The MIC was read after 24 h of incubation at 35°C according to the manufacturer's instructions.

diate effect between the wild type and calcineurin mutants in *C. dubliniensis* (Fig. 3B). This strongly suggests that fluconazole tolerance is controlled by other calcineurin downstream targets in addition to the Crz1 transcription factor.

Time-killing curve assays showed that *C. dubliniensis cna1*/*cna1* and *cnb1*/*cnb1* mutants initially (3 h) proliferated in the presence of fluconazole (10 μg/ml) but that survival was dramatically decreased over 24 h compared with the wild type ($P < 0.0001$; Fig. 3C). *C. dubliniensis crz1*/*crz1* mutants exhibited initial growth, but the growth rate dropped significantly at 24 h ($P < 0.05$; Fig. 3C). The synergistic fungicidal effects of fluconazole are therefore strongly linked to the loss of calcineurin activity and are partially mediated by the transcription factor Crz1. Calcineurin mutants also exhibited hypersusceptibility to the new-generation azoles, posaconazole and voriconazole, in *C. dubliniensis* and *C. albicans*, while *crz1*/*crz1* mutants showed differential susceptibility (see Fig. S4 in the supplemental material). This suggests that azole tolerance is at least in part mediated by the transcription factor Crz1. However, *C. dubliniensis* Crz2 (CD36_32610, encoding a putative transcriptional regulator) does not play a role in azole tolerance because *crz2*/*crz2* and *crz2*/*crz2 crz1*/*crz1* mutants did not exhibit hypersusceptibility compared with the wild type and *crz1*/*crz1* mutants, respectively (data not shown).

Calcineurin and Crz1 control cation homeostasis in *C. dubliniensis*. The roles of calcineurin and Crz1 in Ca^{2+}, Mn^{2+}, or Na^+ cation homeostasis have been elucidated in *C. albicans* (18, 68, 69). Sanglard et al. showed that *C. albicans cna1*/*cna1* mutants are hypersensitive to Ca^{2+} and Na^+ (1.5 M) (68) while *crz1*/*crz1* mutants are hypersensitive to divalent Ca^{2+} and Mn^{2+} (42, 69). In other fungal pathogens, including *C. neoformans* (59), *A. fumigatus* (73), and *Magnaporthe oryzae* (21), calcineurin is required for Ca^{2+} ion homeostasis. Our laboratory previously showed that calcineurin is required for *C. albicans* to survive Ca^{2+} exposure in serum and thereby for virulence (7, 8). These observations suggest a general role for calcineurin in controlling Ca^{2+} homeostasis. Recently, Enjalbert et al. showed that *C. dubliniensis* is Na^+ hypersensitive compared with *C. albicans* (31). Thus, it is of interest to investigate the potential roles of calcineurin in Na^+, Ca^{2+}, and Mn^{2+} homeostasis in *C. dubliniensis*.

Here, we demonstrate that, similarly to *C. albicans*, *C. dubliniensis* calcineurin (Cna1 and Cnb1) and Crz1 are essential for growth in response to Ca^{2+} stress (Fig. 4A). Surprisingly, at elevated temperature (≥30°C), *crz1*/*crz1* mutants are hypersensitive to Ca^{2+} compared with the calcineurin mutants in two closely related species (see Fig. S5 in the supplemental material). Interestingly, *crz1*/*crz1* mutants exhibit intermediate Ca^{2+} sensitivity phenotype compared with wild type and calcineurin mutants at 24°C in both *C. dubliniensis* and *C. albicans* (Fig. S5). *C. dubliniensis cna1*/*cna1* and *cnb1*/*cnb1* mutants are also hypersensitive to Mn^{2+} stress (Fig. 4A), whereas *crz1*/*crz1* mutants exhibit intermediate sensitivity between the calcineurin mutants and wild type, indicating that another regulator(s) in addition to Crz1 contributes to Mn^{2+} homeostasis. Interestingly, *C. dubliniensis* calcineurin mutants are hypersensitive to Na^+ (1 M), while *C. albicans* calcineurin mutants do not exhibit significant differences compared with their wild-type counterparts (Fig. 4A). In fact, *C. albicans* calcineurin mutants are hypersensitive to a high Na^+ concentration (2 M; data not shown). Thus, the difference in roles of calcineurin in Na^+ ion homeostasis between two closely related species (Fig. 4A) is due to the differential Na^+ sensitivity between the species and not to differences in calcineurin activity in the two species.

The mechanisms of *C. dubliniensis* calcineurin and *crz1*/*crz1* mutants' hypersensitivity to mono- or divalent cations might involve defects in cation efflux systems, resulting in cation accumulation in the cytosol. We show here that transcription of *PMC1* (encoding a vacuolar Ca^{2+} transporter, CD36_81200) is regulated by calcineurin and Crz1 in *C. dubliniensis* (Fig. 4B, $P < 0.001$), indicating a mechanism by which Ca^{2+} likely accumulates in the cytosol of calcineurin or *crz1*/*crz1* mutants. The transcription of *PMC1* was also shown to be regulated by calcineurin and Crz1 in *C. albicans* (42, 68) and in the rice blast pathogen *M. oryzae* (20). However, the transcription of *PMR1* (encoding a Golgi Ca^{2+}/Mn^{2+} transporter, CD36_70530), *CCH1* (encoding a voltage-gated Ca^{2+} channel, CD36_01040), and *MID1* (encoding a Ca^{2+} channel, CD36_53710) was not controlled by calcineurin or Crz1 (Fig. 4B) in *C. dubliniensis*.

Calcineurin but not Crz1 is required for serum survival in *C. dubliniensis*. An essential role for calcineurin, but not Crz1, in serum survival has been demonstrated in *C. albicans* (8), and calcium stress in serum has been elucidated to be the cause of lethality of calcineurin mutants (7). An inability to survive in serum explains, at least in part, why *C. albicans* calcineurin mutants exhibit attenuated virulence in a murine systemic in-

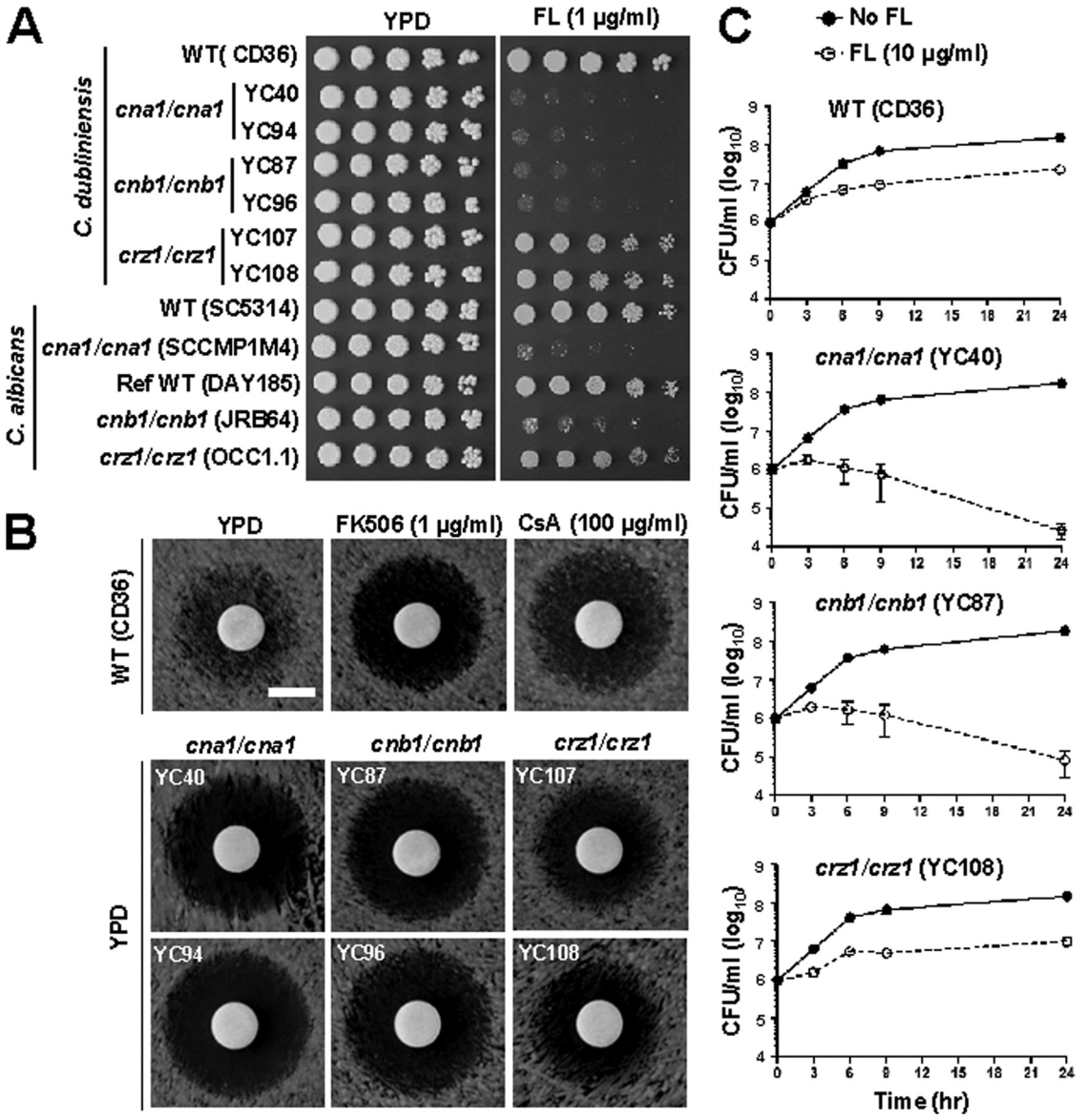

FIG. 3. Calcineurin is required for fluconazole tolerance in *C. dubliniensis*. (A) Cells were grown overnight in YPD at 30°C, 5-fold serially diluted, and spotted onto YPD medium ± fluconazole (FL). The plates were incubated at 30°C for 48 h. (B) Disk diffusion assays were used to determine fluconazole susceptibility of wild-type and mutant strains. Cells were grown overnight at 30°C, and 0.1 OD_{600} (in 100 μl) was spread on the surface of YPD medium ± FK506 or CsA at the concentrations indicated. A disk was placed on the surface of the medium, and fluconazole (1 μg) was added to each disk. The plates were incubated at 30°C for 24 h and photographed. Scale bar = 6 mm. (C) Time-killing curve of wild type and *cna1*/*cna1*, *cnb1*/*cnb1*, and *crz1*/*crz1* mutants in YPD medium ± fluconazole. The data are represented as means ± SDs from triplicate experiments.

fection model but not in pulmonary or vaginal infection models (5), indicative of niche-specific roles of calcineurin. However, the roles of calcineurin and Crz1 have not yet been investigated in the less virulent species *C. dubliniensis*. Here, we demonstrate that, similar but not identical to *C. albicans* calcineurin mutants, *C. dubliniensis cna1*/*cna1* and *cnb1*/*cnb1* mutants were hypersensitive to serum but were in general less sensitive than *C. albicans* calcineurin mutants (Fig. 5A), suggesting an evolutionary divergence between two closely related species. By quantitative measurements, we found that the survival percentage of *C. dubliniensis cna1*/*cna1* mutants (0.354% ± 0.125%) was 24-fold higher than *C. albicans cna1*/*cna1* mutants (0.015% ± 0.006%) ($P = 0.0094$) on a 50% serum agar plate (data not shown). However, Crz1 is not required for serum survival in either *Candida* species (Fig. 5 and data not shown). We further characterized germ tube formation of the wild type and mutants in 100% serum. Similar to the *C. albicans* calcineurin mutant, the *C. dubliniensis* calcineurin mutants exhibit germ tube formation defects at 2 h and further growth was inhibited over 24 h (Fig. 5B). However, *C. dubliniensis* Crz1 is not required for germ tube formation in liquid 100% serum (Fig. 5B). Taken together, calcineurin, but not Crz1, is required for serum survival and germ tube formation in 100% serum in *C. dubliniensis*.

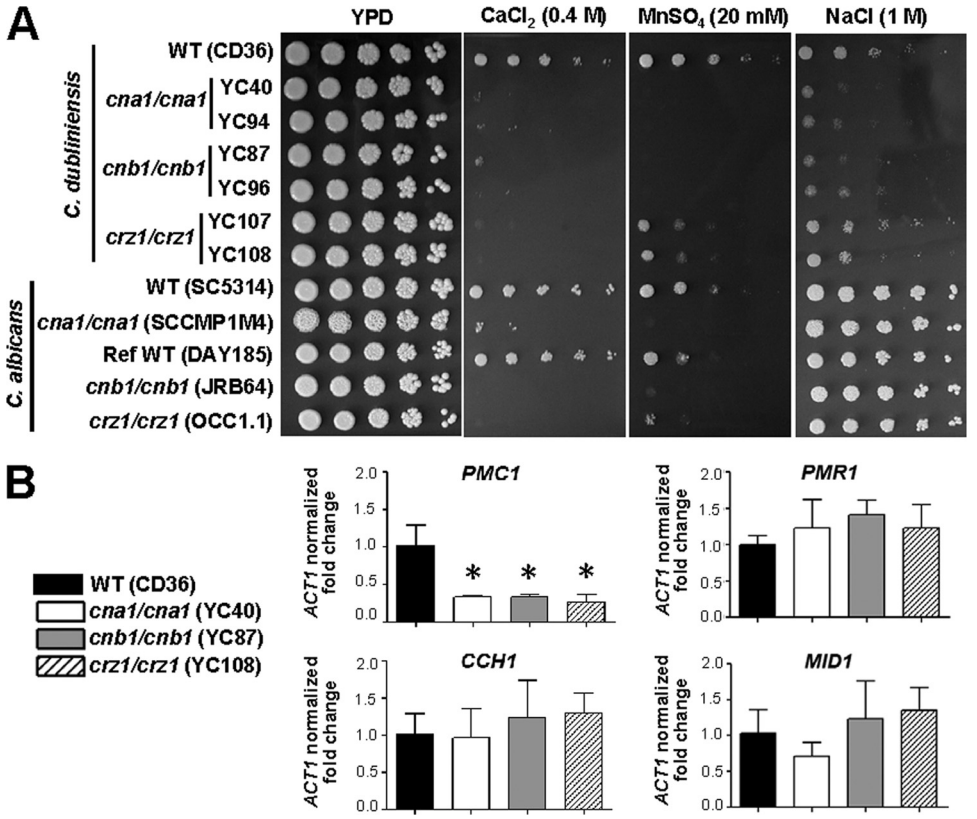

FIG. 4. Calcineurin and Crz1 control cation homeostasis in *C. dubliniensis*. (A) Cells were grown overnight in YPD at 30°C, 5-fold serially diluted, and spotted onto YPD medium containing $CaCl_2$, $MnSO_4$, or NaCl at the concentration indicated. The plates were incubated at 30°C for 48 h. (B) Quantitative real-time PCR was used to assay expression of genes involved in cation homeostasis (*PMC1* and *PMR1*) or calcium channel (*CCH1* and *MID1*) in the wild-type and mutant strains. The fold changes in transcription of each gene were normalized to the endogenous control *ACT1*. The error bars represent means ± SDs from a triplicate experiment. One representative figure of three independent experiments is shown. Asterisks indicate $P < 0.001$ compared with the wild type.

Calcineurin and Crz1 are required for hyphal growth in *C. dubliniensis*. It is unclear if calcineurin is required for hyphal growth in *C. albicans*. Two groups, including our own, found no clear role for calcineurin in hyphal growth (5, 8), while another group suggested that calcineurin and Crz1 may be required for hyphal growth on spider medium (carbon source starvation) (42, 68). Sanglard et al. reported that a *C. albicans cna1*/*cna1* mutant also exhibits attenuated hyphal growth on SLAD medium (nitrogen source starvation) (68). Here, we clarify the roles of calcineurin in *C. dubliniensis* hyphal growth in response to carbon or nitrogen limitation. We found that hyphal growth of *cna1*/*cna1* and *cnb1*/*cnb1* mutants and FK506-treated wild type is severely impaired on solid spider, SLAD, and FA (filament agar; no added nitrogen source) media (Fig. 6), showing a clearly demonstrable role for calcineurin in hyphal growth in response to nutrient deprivation in *C. dubliniensis*. Interestingly, Crz1 is required for hyphal growth during carbon (spider medium) but not nitrogen (SLAD and FA media) starvation in *C. dubliniensis* (Fig. 6). The hyphal growth defects of *C. dubliniensis crz1*/*crz1* mutants on solid spider medium were complemented by introducing the wild-type *CRZ1* gene under the control of its native promoter (see Fig. S2 in the supplemental material). In *C. albicans*, Karababa et al. also reported that *crz1*/*crz1* mutants exhibit hyphal growth defects on solid spider medium, but the roles of *C. albicans* Crz1 in growth on nitrogen-limited medium have not been reported (42, 69). On solid serum agar (50% serum, 2% agar), *C. dubliniensis* calcineurin is integral for growth while Crz1 is not. However, the hyphal growth of *crz1*/*crz1* mutants was attenuated on serum agar compared with the wild-type or complemented strains (Fig. 6 and data not shown), suggesting a specific role of Crz1 in regulating hyphal growth in solid serum agar.

We also found that *C. dubliniensis cna1*/*cna1* and *cnb1*/*cnb1* mutants and FK506-treated wild type but not *crz1*/*crz1* mutants exhibit reduced germ tube formation in liquid spider medium compared with the wild type ($P < 0.01$) (see Fig. S6 in the supplemental material). In contrast, a *C. albicans cna1*/*cna1* mutant or FK506-treated wild-type cells exhibit normal germ tube formation in liquid spider medium (Fig. S6), suggesting that calcineurin function in response to nutrient starvation in liquid may be diverged between the two species. O'Connor et al. recently reported that unlike *C. albicans*, *C. dubliniensis* exhibits differential hyphal growth in response to nutrient starvation (57). Interestingly, *C. dubliniensis* Crz1 shows differential responses to hyphal growth in solid and liquid spider media (Fig. 6; see also Fig. S6). In contrast to defects on solid spider medium, *C. dubliniensis crz1*/*crz1* mutants exhibit normal germ

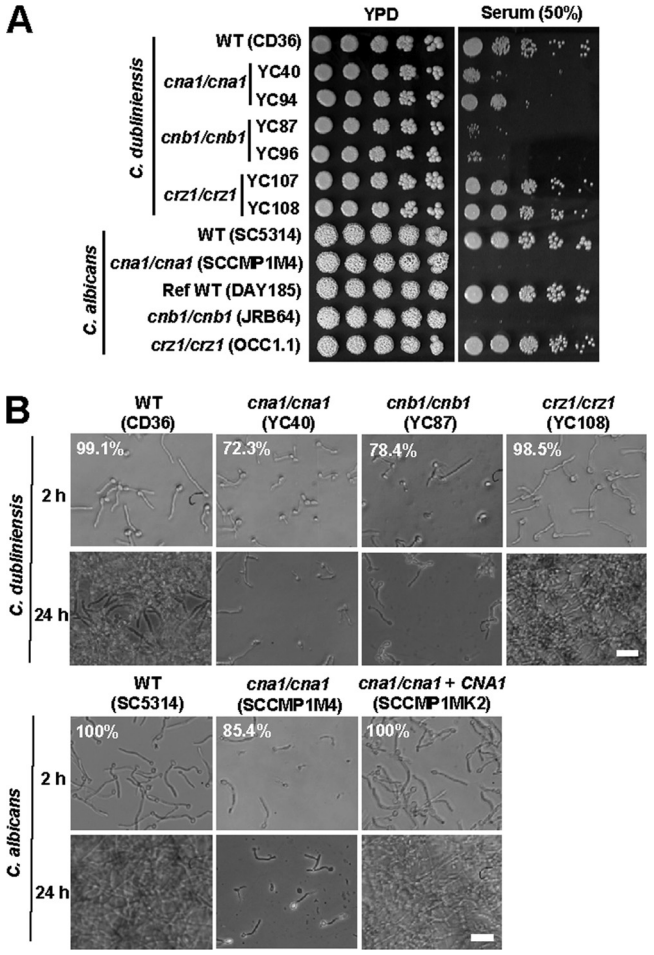

FIG. 5. Calcineurin is required for serum survival in *C. dubliniensis*. (A) Cells were grown overnight in YPD at 30°C, 5-fold serially diluted, and spotted onto YPD or 50% serum agar plates. The plates were incubated at 37°C for 48 h. (B) Germ tube formation of wild-type and mutant strains in the presence of 100% serum. Cultures in the 96-well polystyrene plates were incubated at 37°C statically for the times indicated. The percentage of cells forming germ tubes was determined from at least 200 cells. Scale bar = 40 μm.

tube formation in liquid spider medium compared with wild type (Fig. S6). These lines of evidence show that calcineurin (Cna1 and Cnb1) is required for hyphal growth in response to nutrient starvation, while Crz1 plays different roles dependent upon nutrient starvation and other medium conditions (solid or liquid) in *C. dubliniensis*. These results suggest that the role of calcineurin in hyphal growth of *C. dubliniensis* is, at least in part, mediated by Crz1 in response to various environmental cues.

Thigmotropism is attenuated in the *crz1*/*crz1* mutant. The thigmotropic (contact-sensing) response of fungal hyphae enables the growing tip to circumnavigate impenetrable objects encountered in the environment. In plant pathogens, sensing substrate contours allows fungi to locate and identify the specific topography of penetration sites in the host leaf (1). Contact with an object is proposed to be sensed in *C. albicans* by a mechanism involving activation of plasma membrane calcium channels, which initiates a turning response in the hyphal tip (11, 88). We tested whether calcium signaling through the two calcineurin subunits or the Crz1 transcription factor was required for thigmotropism in *C. dubliniensis*. Because the hyphae of *C. albicans* and *C. dubliniensis* are similar in diameter, we tested the response using the same quartz slides with 0.79-μm ridges. No difference was observed in the thigmotropic response of the *cna1*/*cna1* or the *cnb1*/*cnb1* mutants compared to the wild-type strain, but turning was reduced by approximately one-third in the *crz1*/*crz1* mutant ($P = 0.032$) (Fig. 7). This result is similar to that observed for *C. albicans*, although the effect of the *crz1* mutation compared to the control strain was less marked in *C. dubliniensis*.

The hyphae of filamentous fungi generally grow toward the cathode in an applied electric field (galvanotropism) (25). In *C. albicans*, deletion of *CNA1*, *CNB1*, or *CRZ1* resulted in the attenuation of the galvanotropic response (11). However, we were unable to test the response of *C. dubliniensis* using this assay due to its failure to generate hyphae on application of an electric field of 10 V/cm^{-1}, although the cells remained viable in a field applied for 6 h and grew as normal in the medium used when no field was present. One possibility is that the field generated an electrolytic product that inhibited growth in *C. dubliniensis* but was not fungicidal.

Deletion of calcineurin and Crz1 attenuates virulence in mice. *C. dubliniensis* is generally considered to be a less pathogenic species compared to *C. albicans* (77). However, it has also been reported that *C. dubliniensis* can be more virulent than *C. albicans* in a murine systemic infection model (35, 85). Here, we used *C. albicans* as the control group to compare its virulence to *C. dubliniensis* and determined the virulence of calcineurin and *crz1*/*crz1* mutants of *C. dubliniensis* in a murine systemic infection model. The median animal survival following tail vein infection with 5×10^6 cells is 20 days for *C. dubliniensis* and 2 days for *C. albicans*, respectively, showing a dramatic virulence difference ($P < 0.0001$) between these two *Candida* species. In *C. albicans*, *cna1*/*cna1* and *cnb1*/*cnb1* mutants exhibit strongly attenuated virulence (4, 5, 8, 68), while *crz1*/*crz1* mutants have either full (62) or slightly reduced (42) virulence in a murine systemic infection model. Here we showed that *C. dubliniensis cna1*/*cna1* (YC40 and YC94) or *cnb1*/*cnb1* (YC87 and YC96) mutants exhibit strongly attenuated virulence compared with the wild type ($P < 0.0001$) (Fig. 8A) while *crz1*/*crz1* mutants (YC107 and YC108) exhibit attenuated virulence compared with the wild type ($P < 0.002$). However, there is no statistically significant difference between calcineurin and *crz1*/*crz1* mutant-infected mice ($P > 0.3$), indicating that both calcineurin and Crz1 affect the virulence of *C. dubliniensis*.

To determine colonization ability, we performed kidney fungal burden analysis of animals infected with wild type and the mutants. *cna1*/*cna1* mutants (YC40 and YC94) exhibited 42-fold-reduced fungal burden in the kidneys compared with the wild type ($P < 0.01$) (Fig. 8B). In contrast, the difference of fungal burden between *cnb1*/*cnb1* mutants (YC87 and YC96) and wild type was less pronounced ($P = 0.08$) (Fig. 8B). One *cnb1*/*cnb1* mutant (YC96) exhibited a 44-fold-reduced fungal burden compared with wild type ($P = 0.02$), while another *cnb1*/*cnb1* mutant (YC87) exhibited a 2.8-fold (lower fold change is attributable to a single outlier)-reduced fungal burden compared with wild type ($P = 0.2$) (Fig. 8B). When the

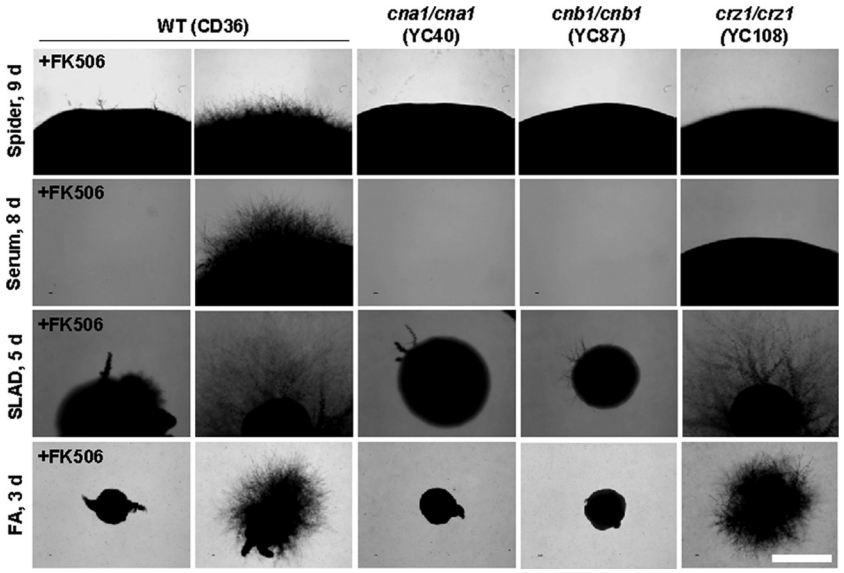

FIG. 6. Calcineurin controls colony hyphal growth in *C. dubliniensis*. Cells were grown overnight and washed twice with ddH_2O. Cells were separated by sonication, counted with a hemocytometer, and then serially diluted to 10^3 cells/ml. One hundred microliters containing ~100 cells was spread on a variety of filament-inducing media ± FK506 (1 μg/ml) and incubated at 37°C for the number of days indicated. The experiments were repeated at least three times, and one representative image is shown. Scale bar = 1 mm.

outlier animal from the YC87 infection is excluded from the analysis, the *cnb1*/*cnb1* mutants (YC87 and YC96) exhibited a 42-fold-reduced fungal burden compared with the wild type ($P = 0.01$). The fungal burden of mice infected with *crz1*/*crz1* mutants (YC107 and YC108) was 3.4-fold reduced compared with the wild type ($P = 0.09$) (Fig. 8B). Taken together, mice infected with *C. dubliniensis* calcineurin and *crz1*/*crz1* mutants exhibited a reduced fungal burden overall compared with the wild type.

In histopathological analysis, GMS-stained tissues revealed that the wild type readily forms hyphae and proliferates extensively in tissues around the renal pelvis, while cells of the *cna1*/*cna1*, *cnb1*/*cnb1*, and *crz1*/*crz1* mutants were not observed (Fig. 8C), indicating that hyphal growth may be reduced *in vivo* for the calcineurin pathway mutants. In the H&E staining, tissue damage or necrosis was observed only in animals infected with the wild type and not with the calcineurin or *crz1*/*crz1* mutants (Fig. 8C).

Calcineurin mutants are unable to establish murine ocular infection. *Candida* species were isolated from AIDS patients with corneal infections (keratitis) (38, 39). *Candida* keratitis caused by *C. albicans* and NACS, including *Candida glabrata* and *Candida parapsilosis* (16, 81), continues to be an important cause of ocular morbidity, including loss of vision. Although *C. dubliniensis* is frequently found in AIDS patients, it is unclear if *C. dubliniensis* has the ability to cause keratitis of patients.

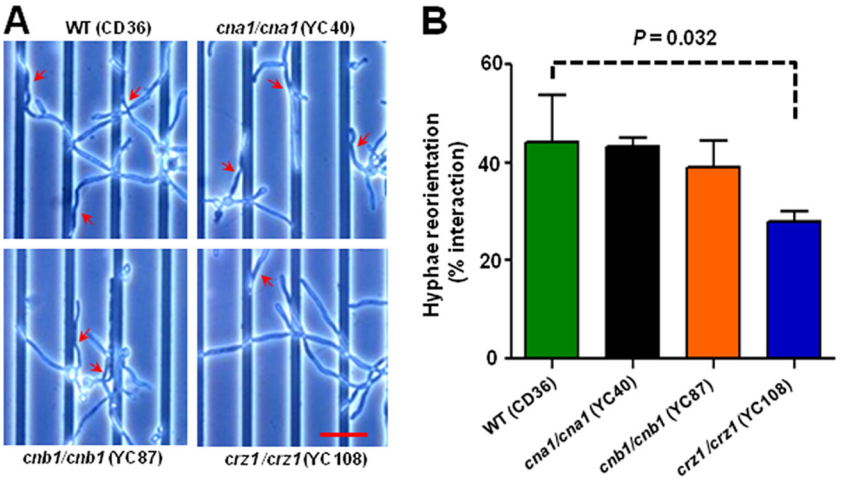

FIG. 7. The thigmotropic response is attenuated in *C. dubliniensis crz1*/*crz1* but not calcineurin mutants. (A) The thigmotropic response was determined when the growing tip reoriented against 0.79-μm ridges in the substrate. The turning hyphae are indicated by arrowheads. Scale bar = 25 μm. One representative figure from three independent experiments is shown. (B) Bar graph shows the percentage of total hyphae that reorientated. The error bars represent the means ± SDs.

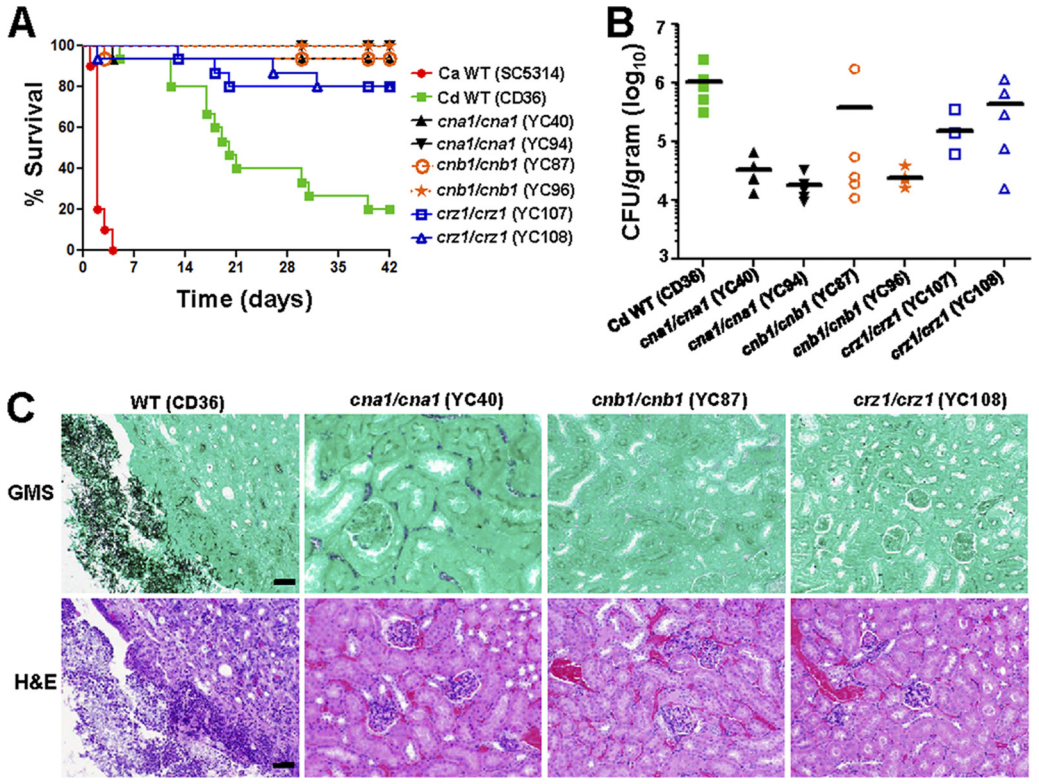

FIG. 8. Calcineurin and *crz1*/*crz1 C. dubliniensis* mutants are compromised for virulence in a murine systemic infection model. (A) The survival of mice following intravenous challenge with 5×10^6 *C. dubliniensis* (Cd) or *C. albicans* (Ca) yeast cells was monitored for up to 42 days. Fifteen mice per strain were used for all strains except *C. albicans* wild type (10 mice). (B) The fungal burden in the kidneys was determined at day 7 after challenge. Five mice per strain were used for all strains except YC107 (4 mice were analyzed because one animal died immediately after infection). (C) Histopathological sections of kidneys dissected from mice infected with wild-type or *cna1*/*cna1*, *cnb1*/*cnb1*, or *crz1*/*crz1* mutant strains. The mice were challenged with 5×10^6 yeast cells and sacrificed at day 14. GMS and H&E stains were used to observe *C. dubliniensis* colonization and tissue necrosis, respectively. Scale bar = 50 μm.

The comparison of virulence between *C. albicans* and *C. dubliniensis* in murine ocular infection has not yet been reported. We here investigate the virulence difference between these two closely related species and test if calcineurin promotes ocular infection in *C. dubliniensis*. Mice infected with an inoculum of 10^6 cells of *C. albicans* exhibited visible opacity and surface opacity in immunocompetent ICR mice (100%, 15/15). However, *C. dubliniensis* at an inoculum of 10^6 did not result in persistent manifestation of fungal keratitis in immunocompetent mice, suggesting that *C. dubliniensis* is less virulent in murine ocular infection. An immunocompromised mouse model for fungal keratitis is well established for *C. albicans* (60, 89) but not yet tested for *C. dubliniensis*. We thus administered cyclophosphamide (180 to 220 mg/kg body weight), a potent inhibitor of lymphocyte proliferation, to mice on days 5, 3, and 1 prior to inoculation. All corneas (100%, 15/15) infected with 10^6 cells of *C. albicans* SC5314 developed fungal keratitis compared to 26.7% (4/15) of those exposed to *C. dubliniensis* CD36 (Fig. 9A). At all time points, keratitis caused by *C. albicans* SC5314 was more severe than that caused by *C. dubliniensis* CD36 (Fig. 9B). The disease score of *C. albicans* keratitis is persistent, while *C. dubliniensis* keratitis has a peak at day 3 but drops subsequently, suggesting that *C. dubliniensis* is not a successful pathogen compared to its closely related species *C. albicans*. This is the first demonstration that compares these two species using a fungal keratitis model.

Corneas infected with *C. dubliniensis* CD36 wild type (26.7%, 4/15) and *crz1*/*crz1* mutant (22.2%, 4/18), but not calcineurin mutants (*cna1*/*cna1* and *cnb1*/*cnb1*), showed visible keratitis (Fig. 9), suggesting that *C. dubliniensis* calcineurin is required for establishing murine ocular infection. The mean keratitis score for the CD36 wild-type strain was similar to the *crz1*/*crz1* mutant. Keratitis caused by CD36 was moderate grade by day 1 (6.25 ± 0.96) and became more severe by day 3 (8.00 ± 0.82, $P = 0.033$) with inflammation starting to resolve by day 4 (5.75 ± 1.26) (Fig. 9B). Fungal keratitis resulting from the *crz1*/*crz1* mutant started to resolve by day 3 and was significantly different by day 6 ($P = 0.027$) compared with the CD36 strain at day 6 (Fig. 9B), suggesting a difference between CD36 and *crz1*/*crz1* mutant in developing keratitis at later stages. Compared with the CD36 wild-type and *crz1*/*crz1* mutant strains, it is clear that *C. dubliniensis* calcineurin mutants are unable to establish murine ocular infection (Fig. 9), supporting our previous finding that *C. albicans* calcineurin mutants exhibit attenuated virulence in a fungal keratitis model (60).

Calcineurin is required for biofilm formation in a rat denture model. In addition to *C. albicans* and *C. glabrata* (23), *C.*

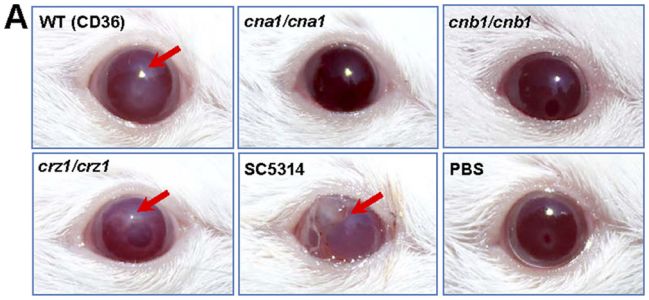

Visible keratitis

WT (CD36)	cna1/cna1	cnb1/cnb1	crz1/crz1	SC5314	PBS
26.7% (4/15)	0% (0/15)	0% (0/16)	22.2% (4/18)	100% (15/15)	0% (0/13)

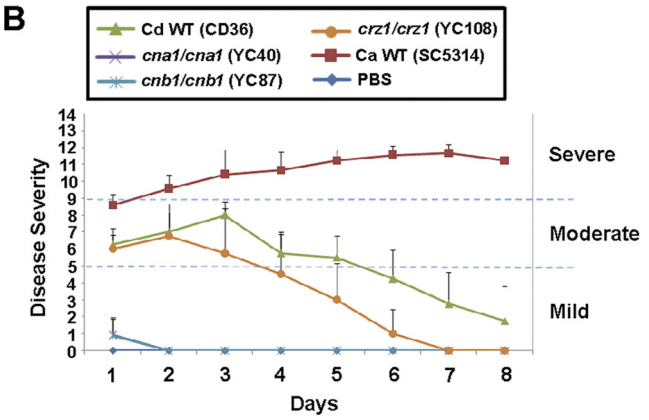

FIG. 9. *C. dubliniensis* calcineurin mutants are unable to establish murine ocular infection. (A) Clinical photographs of corneas of immunosuppressed (cyclophosphamide-treated) mice 2 days after the inoculation of 10^6 yeast cells. Fungal keratitis, indicated by red arrows, was seen only in animals infected with *C. albicans* SC5314 (100%, 15/15), *C. dubliniensis* CD36 (26.7%, 4/15), and *crz1*/*crz1* mutant (YC108, 22.2%, 4/18). (B) Each cornea of an immunosuppressed mouse was inoculated with 10^6 yeast cells of each strain, and the disease severity was scored for 8 days. *C. albicans* SC5314 served as a reference control. Mice infected with *C. dubliniensis cna1*/*cna1* or *cnb1*/*cnb1* mutants or the PBS control exhibited normal cornea, and score curves essentially overlapped. Mice infected with *C. albicans* SC5314 and *C. dubliniensis* wild-type CD36 and *crz1*/*crz1* mutant strains, exhibiting visible signs of keratitis, were plotted.

dubliniensis is frequently isolated from denture wearers who present with or without denture-related stomatitis (34, 48). *Candida* species can form azole-resistant biofilms on dentures, in which treatment is difficult. However, knowledge regarding the role of *C. dubliniensis* in denture biofilm formation is limited. Therefore, it will be useful to have a denture biofilm model to examine *C. dubliniensis* biofilm formation and investigate calcineurin as a potential drug target. A rat denture model was chosen for an *in vivo* biofilm infection model (54). After 48 h of growth, the *C. dubliniensis* wild-type (CD36) strain produced a biofilm spanning a majority of the inoculated denture surface consisting of yeast, hyphae, and matrix components (Fig. 10). In contrast, inoculation of the *cna1*/*cna1* mutant resulted in only a yeast monolayer (Fig. 10), suggesting that calcineurin is required for hyphal growth in an *in vivo* denture biofilm model and could be targeted for therapeutic purposes.

DISCUSSION

Roles of calcineurin and Crz1 in cell wall integrity and drug tolerance. Here we demonstrate that calcineurin and Crz1 control cell wall integrity and drug tolerance in *C. dubliniensis*, suggesting potential merit for calcineurin inhibitors as novel therapeutic agents. Most antifungal drugs target fungal protein components on either the cell membrane or cell wall. For example, azoles inhibit ergosterol biosynthesis in the cell membrane, and echinocandins inhibit β-1,3-glucan biosynthesis in the cell wall (58). In *C. albicans* and *C. glabrata*, calcineurin is required for cell wall integrity (26, 50). The cell membrane or wall defects caused by calcineurin mutation render antifungal azoles fungicidal in *C. albicans* (26). Here we show that cell membrane/wall integrity is partially mediated by Crz1 in *C. dubliniensis*; *crz1*/*crz1* mutants exhibit SDS hypersensitivity intermediate between the wild type and calcineurin mutants (Fig. 1B). However, *C. dubliniensis* Crz1 does not play a clear role in response to cell wall perturbation by CFW and Congo red (Fig. 1B). These lines of evidence suggest that calcineurin plays an important role governing cell wall integrity which might involve other cell wall integrity pathways such as the protein kinase C (PKC) and high-osmolarity glycerol (HOG) signaling pathways.

In *C. albicans*, cell membrane perturbation by fluconazole can enhance uptake and toxicity of calcineurin inhibitors (26). Conversely, it is possible that cell membrane defects caused by calcineurin mutation result in increased azole uptake and toxicity, leading to synergistic fungicidal activity. Roles for calcineurin and Crz1 in azole (26, 68) or echinocandin (70) tolerance have been studied in *C. albicans*. However, data showing interactions between calcineurin and other signaling pathways to regulate drug tolerance are limited. Singh et al. demonstrated that heat shock protein 90 (Hsp90) physically interacts with calcineurin and governs echinocandin resistance in *C. albicans*, and drug inhibitors of Hsp90 or calcineurin exhibit synergistic fungicidal activity with echinocandins (at a nonfungicidal concentration) (70). Recently, LaFayette et al. showed that PKC signaling regulates azole and echinocandin tolerance via circuits comprised of calcineurin, Hsp90, and Mkc1 in *C. albicans* (46). It is possible that *C. dubliniensis* shares these conserved pathways that may function in coordination with the calcineurin pathway to effect cell wall integrity and drug tolerance.

Roles of calcineurin and Crz1 in hyphal growth and contact response orientation. In *C. albicans*, the roles of calcineurin in hyphal growth are unclear; two groups, including our own, were unable to find a role for calcineurin in hyphal growth (5, 26), while another group reported that a calcineurin mutant (*cna1*/*cna1*) exhibited hyphal growth defects on spider and SLAD solid media (68) (Table 3). The contrasting results regarding the roles of the calcineurin pathway in hyphal growth of *C. albicans* may be due to different *C. albicans* backgrounds or experimental details. In this study, we aimed to use *C. dubliniensis*, a species closely related to *C. albicans*, to investigate the roles of calcineurin (Cna1 and Cnb1) in hyphal growth, a phenotype linked to virulence. We find that calcineu-

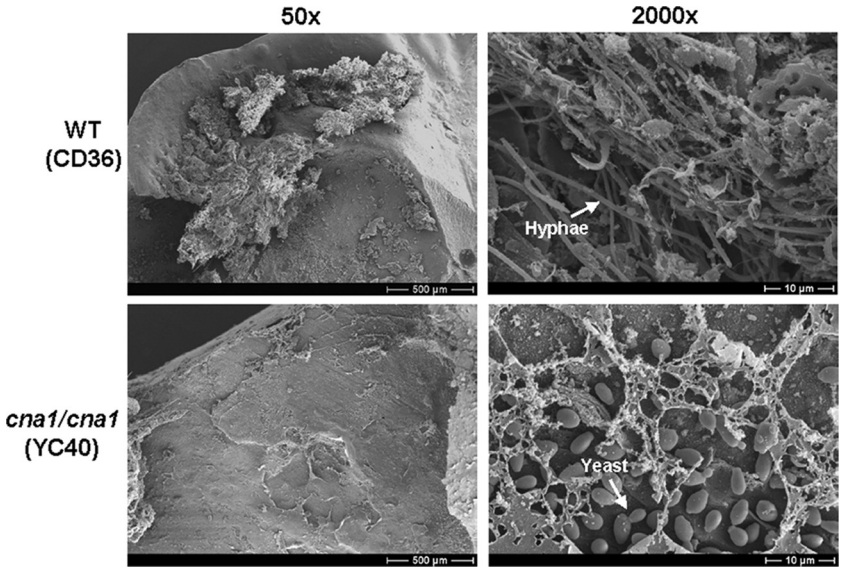

FIG. 10. Scanning electron microscopy (SEM) images of a *C. dubliniensis* rat denture biofilm model. Rat dentures were harvested after 48 h of growth, processed for SEM, and imaged. Scale bars for 50× and 2,000× images represent 500 μM and 10 μM, respectively.

rin (Cna1 or Cnb1) is clearly required for hyphal growth in response to either carbon or nitrogen source limitation in *C. dubliniensis* (Fig. 6; Table 3). However, in *C. albicans* we are unable to appreciate a clear role for calcineurin in hyphal growth upon either carbon or nitrogen source starvation.

In *C. albicans*, the roles of the transcription factor Crz1 in hyphal growth remain elusive. Karababa et al. reported that Crz1 is required for hyphal growth on spider medium (42), while Noble et al. showed that *crz1*/*crz1* mutants exhibited no hyphal growth defects on spider medium from a systematic

TABLE 3. Summary of *C. albicans* and *C. dubliniensis* calcineurin and *crz1*/*crz1* mutant phenotypes

Phenotype	*C. albicans*		*C. dubliniensis*	
	Calcineurin	*crz1*/*crz1*	Calcineurin	*crz1*/*crz1*
Cell wall integrity				
SDS	Inviable	Intermediate[a]	Inviable	Intermediate[a]
CFW	Sensitive	Wild type	Hypersensitive	Wild type
Congo red	Wild type	Wild type	Hypersensitive	Wild type
Drug tolerance				
Echinocandin	Hypersusceptible	Differential[b]	Hypersusceptible	Differential[b]
Azole	Hypersusceptible	Intermediate	Hypersusceptible	Intermediate
Ion homeostasis				
Ca^{2+}	Hypersensitive[c]	Hypersensitive	Hypersensitive[c]	Hypersensitive
Mn^{2+}	Hypersensitive	Hypersensitive	Hypersensitive	Hypersensitive
Na^{+}	Hypersensitive[d]	Wild type	Hypersensitive[e]	Wild type
Serum survival	Hypersensitive	Wild type	Sensitive	Wild type
Hyphal growth (solid surface)				
Carbon limitation	Wild type	Wild type	Impaired	Impaired
Nitrogen limitation	Wild type	Wild type	Impaired	Wild type
Tropic responses				
Thigmotropism	Wild type	Attenuated	Wild type	Attenuated
Galvanotropism	Attenuated	Attenuated	NA[f]	NA[f]
Virulence (murine systemic infection)	Attenuated	Wild type/attenuated	Attenuated	Attenuated

[a] Intermediate phenotype between wild type and calcineurin mutants.
[b] Mutants exhibit either no response or intermediate susceptibility to echinocandins.
[c] These observations were found at 24 and 30°C (0.4 M). Interestingly, *C. albicans* mutants exhibit the wild-type phenotype while *C. dubliniensis* mutants exhibit the sensitive phenotype at 37°C (see Fig. S5 in the supplemental material).
[d] Hypersensitivity at 2 M NaCl.
[e] Hypersensitivity at 1 M NaCl.
[f] Failure to generate hyphae when an electric field was applied.

screen (55). The confounding results may be due to different experimental methods or genetic backgrounds of *C. albicans* strains. However, the calcineurin target CrzA in *A. fumigatus* has been demonstrated to regulate hyphal growth (24), indicative of a potential global role of the calcineurin target Crz1/CrzA in regulating hyphal growth in fungal pathogens. In support of the interpretation that Crz1 is a global regulator of hyphal growth, we find that Crz1 is required for hyphal growth on solid spider and serum media in *C. dubliniensis* (Fig. 6). However, *C. dubliniensis* Crz1 is not required for germ tube formation in either liquid spider or serum medium (Fig. 5; see also Fig. S6 in the supplemental material), indicating a fascinating role for Crz1 in adhering to a solid surface.

Brand et al. demonstrated that hyphal orientation (thigmotropism or galvanotropism) is linked to the calcium signaling and calcineurin pathway in *C. albicans* (9–11). We observed that thigmotropism was reduced in *C. dubliniensis* (CD36) by 25 to 30% compared with *C. albicans* (SC5314) (data not shown). The defective thigmotropism in the *C. dubliniensis crz1*/*crz1* mutant but not calcineurin mutants is consistent with the findings that thigmotropism is mediated by Crz1 in *C. albicans* (11) (Table 3). In *C. albicans*, loss of the thigmotropic response correlated with reduced tissue penetration and damage of oral epithelial cells in an *in vitro* assay (12). Thus, the attenuated thigmotropism of *C. dubliniensis crz1*/*crz1* mutants may partly explain their attenuated virulence in a murine systemic infection model (Fig. 7), but thigmotropism does not appear to contribute to the attenuated virulence of the *C. albicans* and *C. dubliniensis* calcineurin mutants, in which attenuated virulence may simply be due to the essential role of calcineurin for survival in serum in both species.

Role of calcineurin and Crz1 in serum survival and virulence. Fungal pathogens require calcineurin for virulence, but the precise role of calcineurin is species dependent (18). The roles of calcineurin in serum survival have been demonstrated in the human fungal pathogens *C. albicans* (7) and *A. fumigatus* (73). In contrast, in *C. neoformans* calcineurin supports growth at mammalian body temperature (37°C) (59). The plant fungal pathogens *M. oryzae* (21) and *Ustilago maydis* (29) have adapted calcineurin for different pathogenic mechanisms involving appressorial formation and filamentous growth, respectively (18). Here we demonstrate that calcineurin is required for serum survival in *C. dubliniensis* (Fig. 5) and, as a consequence, calcineurin mutants (*cna1*/*cna1* and *cnb1*/*cnb1*) exhibit attenuated virulence (Fig. 8). The requirement for calcineurin in hyphal growth and cell wall integrity suggests additional mechanisms by which calcineurin promotes successful infection. Strikingly, *C. dubliniensis* Crz1 is required for hyphal growth (Fig. 6) and virulence in a murine systemic infection model but is not required for serum survival (Fig. 5), suggesting that Crz1 and calcineurin may contribute to virulence by both common and distinct pathways. In accord with our observations is the fact that defects in cell wall integrity of *C. albicans* often result in attenuated virulence in murine systemic infection models (19, 46, 51).

Our studies also demonstrate that, similar to *C. albicans* and *Saccharomyces cerevisiae*, *C. dubliniensis* calcineurin and Crz1 are not required for growth at high temperature (see Fig. S3 in the supplemental material). Thus, calcineurin in *C. dubliniensis* does not control virulence through promoting high-temperature growth, in contrast to the basidiomycete *C. neoformans*, in which calcineurin is essential for survival at host body temperature (59). In addition to temperature sensitivity, a *Schizosaccharomyces pombe* calcineurin mutant (*ppb1*) exhibits a cold-sensitive phenotype associated with cytokinesis defects (91). It remains largely unknown how calcineurin controls responses to thermal stress in model or pathogenic fungi.

C. dubliniensis has been isolated from nonhuman sources such as seabird-associated excrement or ticks, suggesting that the wax moth (*G. mellonella*) might be a candidate virulence model for *C. dubliniensis*. Interestingly, we found that *C. dubliniensis* is as virulent as *C. albicans* in the *G. mellonella* insect model ($P = 0.32$; see Fig. S7 in the supplemental material), in contrast to their marked virulence difference in the murine model. All wax moth larvae were dead by day 3, when injected with 10^6 *C. dubliniensis* (CD36) yeast cells ($P < 0.0001$, compared with PBS curve) (Fig. S7), indicating that *C. dubliniensis* might be an insect pathogen. However, the roles of calcineurin and Crz1 in virulence in this insect model do not completely phenocopy the murine model (data not shown), suggesting that a specific niche might be required for the *C. dubliniensis* calcineurin pathway to be operative during successful infection.

C. dubliniensis is frequently found in the oral cavities of HIV/AIDS patients; however, its role in this specific niche is unclear. To test if *C. dubliniensis* (CD36) grows and causes damage to oral epithelium, we used FaDu oral epithelial cells to analyze cell-host interactions. We found that *C. dubliniensis* exhibits less extensive hyphal growth compared with *C. albicans* (see Fig. S8A in the supplemental material). Spiering et al. showed that *C. dubliniensis* grew as yeast for the duration of the experiment (12 h) in infected reconstituted human oral epithelium (RHE) (71). We used a ^{51}Cr release assay to determine if *C. dubliniensis* causes cell damage. We found that *C. dubliniensis* causes no damage while *C. albicans* triggers damage within 6 h (Fig. S8B). This suggests that *C. dubliniensis* might have lost virulence determinants that are necessary to colonize oral epithelial cells from *C. albicans*.

Although there are no published clinical reports of keratitis caused by *C. dubliniensis*, it is possible that *C. dubliniensis* could be an emerging and opportunistic pathogen and cause ocular infection when the host immune system is compromised. Our keratitis data support this possibility because *C. dubliniensis* can cause keratitis in an immunocompromised host model. Our lab has demonstrated that CsA and fluconazole exhibit fungicidal activity against *C. albicans* in a murine ocular infection model (60), suggesting a potential combination therapy for keratitis caused by *Candida* species.

A summary of the phenotypes of the *C. dubliniensis* and *C. albicans* calcineurin and *crz1*/*crz1* mutants is shown in Table 3. The *C. dubliniensis* calcineurin pathway exhibits both conserved and distinct roles compared with *C. albicans*. Taken together, the mechanisms linking calcineurin to *C. dubliniensis* pathogenesis involve serum survival and hyphal growth, whereas the virulence impairment of *crz1*/*crz1* mutants may be attributable to their defect in hyphal growth. However, it is possible that other factors such as cell wall integrity may also contribute to calcineurin and Crz1 effects on pathogenicity. These lines of evidence suggest that calcineurin could be a potential drug target in the emerging NACS *C. dubliniensis*.

ACKNOWLEDGMENTS

We thank Lukasz Kozubowski, Cecelia Shertz, and Joanne Kingsbury for comments on the manuscript. We appreciate members of the Heitman and Cardenas labs for helpful discussions. We thank Michael Lorenz for providing the *C. dubliniensis* strain CD36 (original source, Bernard Dujon); Derek Sullivan and Gary Moran for advice on *C. dubliniensis* studies; William Steinbach for caspofungin, micafungin, and anidulafungin; Mitchell Mutz for posaconazole and voriconazole; Dominique Sanglard for *C. albicans* calcineurin and *crz1*/*crz1* mutants; Alice Bungay and Marilou Nicolas for assistance with murine ocular infection studies; and Joachim Morschhäuser for providing the *SAT1* flipper cassette for gene disruptions as well as *C. albicans* strains.

This research was supported by the Duke University Center for AIDS Research (CFAR grant 2P30 AI064518-06 to Y.-L. Chen), NIH-funded program P30 AI64518 to Duke University, and NIH/NIAID R01 grants AI42159 and AI50438 (to J. Heitman). S. G. Filler and N. V. Solis were supported in part by NIH grant R01DE017088.

REFERENCES

1. **Allen, E. A., H. C. Hoch, J. R. Stavely, and J. R. Steadman.** 1991. Uniformity among races of *Uromyces appendiculatus* in response to topographical signalling for appressorium formation. Phytopathology **81:**883–887.
2. **Andes, D., et al.** 2004. Development and characterization of an in vivo central venous catheter *Candida albicans* biofilm model. Infect. Immun. **72:**6023–6031.
3. **Aramburu, J., J. Heitman, and G. R. Crabtree.** 2004. Calcineurin: a central controller of signalling in eukaryotes. EMBO Rep. **5:**343–348.
4. **Bader, T., B. Bodendorfer, K. Schroppel, and J. Morschhauser.** 2003. Calcineurin is essential for virulence in *Candida albicans*. Infect. Immun. **71:** 5344–5354.
5. **Bader, T., et al.** 2006. Role of calcineurin in stress resistance, morphogenesis, and virulence of a *Candida albicans* wild-type strain. Infect. Immun. **74:**4366–4369.
6. **Badiee, P., A. Alborzi, M. A. Davarpanah, and E. Shakiba.** 2010. Distributions and antifungal susceptibility of *Candida* species from mucosal sites in HIV positive patients. Arch. Iran. Med. **13:**282–287.
7. **Blankenship, J. R., and J. Heitman.** 2005. Calcineurin is required for *Candida albicans* to survive calcium stress in serum. Infect. Immun. **73:**5767–5774.
8. **Blankenship, J. R., et al.** 2003. Calcineurin is essential for *Candida albicans* survival in serum and virulence. Eukaryot. Cell **2:**422–430.
9. **Brand, A., and N. A. Gow.** 2009. Mechanisms of hypha orientation of fungi. Curr. Opin. Microbiol. **12:**350–357.
10. **Brand, A., K. Lee, V. Veses, and N. A. Gow.** 2009. Calcium homeostasis is required for contact-dependent helical and sinusoidal tip growth in *Candida albicans* hyphae. Mol. Microbiol. **71:**1155–1164.
11. **Brand, A., et al.** 2007. Hyphal orientation of *Candida albicans* is regulated by a calcium-dependent mechanism. Curr. Biol. **17:**347–352.
12. **Brand, A., et al.** 2008. An internal polarity landmark is important for externally induced hyphal behaviors in *Candida albicans*. Eukaryot. Cell **7:**712–720.
13. **Brandt, M. E., et al.** 2000. *Candida dubliniensis* fungemia: the first four cases in North America. Emerg. Infect. Dis. **6:**46–49.
14. **Braun, B. R., and A. D. Johnson.** 1997. Control of filament formation in *Candida albicans* by the transcriptional repressor TUP1. Science **277:**105–109.
15. **Calderone, R. A., and W. A. Fonzi.** 2001. Virulence factors of *Candida albicans*. Trends Microbiol. **9:**327–335.
16. **Chen, W. L., Y. Y. Tsai, J. M. Lin, and C. C. Chiang.** 2009. Unilateral *Candida parapsilosis* interface keratitis after laser in situ keratomileusis: case report and review of the literature. Cornea **28:**105–107.
17. **Chen, Y. L., S. Kauffman, and T. B. Reynolds.** 2008. *Candida albicans* uses multiple mechanisms to acquire the essential metabolite inositol during infection. Infect. Immun. **76:**2793–2801.
18. **Chen, Y. L., L. Kozubowski, M. E. Cardenas, and J. Heitman.** 2010. On the roles of calcineurin in fungal growth and pathogenesis. Curr. Fungal Infect. Rep. **4:**244–255.
19. **Chen, Y. L., et al.** 2010. Phosphatidylserine synthase and phosphatidylserine decarboxylase are essential for cell wall integrity and virulence in *Candida albicans*. Mol. Microbiol. **75:**1112–1132.
20. **Choi, J., Y. Kim, S. Kim, J. Park, and Y. H. Lee.** 2009. *MoCRZ1*, a gene encoding a calcineurin-responsive transcription factor, regulates fungal growth and pathogenicity of *Magnaporthe oryzae*. Fungal Genet. Biol. **46:** 243–254.
21. **Choi, J. H., Y. Kim, and Y. H. Lee.** 2009. Functional analysis of *MCNA*, a gene encoding a catalytic subunit of calcineurin, in the rice blast fungus *Magnaporthe oryzae*. J. Microbiol. Biotechnol. **19:**11–16.
22. **Chunchanur, S. K., et al.** 2009. Detection and antifungal susceptibility testing of oral *Candida dubliniensis* from human immunodeficiency virus-infected patients. Indian J. Pathol. Microbiol. **52:**501–504.
23. **Coco, B. J., et al.** 2008. Mixed *Candida albicans* and *Candida glabrata* populations associated with the pathogenesis of denture stomatitis. Oral Microbiol. Immunol. **23:**377–383.
24. **Cramer, R. A., Jr., et al.** 2008. Calcineurin target CrzA regulates conidial germination, hyphal growth, and pathogenesis of *Aspergillus fumigatus*. Eukaryot. Cell **7:**1085–1097.
25. **Crombie, T., N. A. Gow, and G. W. Gooday.** 1990. Influence of applied electrical fields on yeast and hyphal growth of *Candida albicans*. J. Gen. Microbiol. **136:**311–317.
26. **Cruz, M. C., et al.** 2002. Calcineurin is essential for survival during membrane stress in *Candida albicans*. EMBO J. **21:**546–559.
27. **Davis, D., R. B. Wilson, and A. P. Mitchell.** 2000. RIM101-dependent and-independent pathways govern pH responses in *Candida albicans*. Mol. Cell. Biol. **20:**971–978.
28. **Del Poeta, M., M. C. Cruz, M. E. Cardenas, J. R. Perfect, and J. Heitman.** 2000. Synergistic antifungal activities of bafilomycin A(1), fluconazole, and the pneumocandin MK-0991/caspofungin acetate (L-743,873) with calcineurin inhibitors FK506 and L-685,818 against *Cryptococcus neoformans*. Antimicrob. Agents Chemother. **44:**739–746.
29. **Egan, J. D., M. D. Garcia-Pedrajas, D. L. Andrews, and S. E. Gold.** 2009. Calcineurin is an antagonist to PKA protein phosphorylation required for postmating filamentation and virulence, while PP2A is required for viability in *Ustilago maydis*. Mol. Plant Microbe Interact. **22:**1293–1301.
30. **Elorza, M. V., H. Rico, and R. Sentandreu.** 1983. Calcofluor white alters the assembly of chitin fibrils in *Saccharomyces cerevisiae* and *Candida albicans* cells. J. Gen. Microbiol. **129:**1577–1582.
31. **Enjalbert, B., et al.** 2009. Genome-wide gene expression profiling and a forward genetic screen show that differential expression of the sodium ion transporter Ena21 contributes to the differential tolerance of *Candida albicans* and *Candida dubliniensis* to osmotic stress. Mol. Microbiol. **72:**216–228.
32. **Fonzi, W. A., and M. Y. Irwin.** 1993. Isogenic strain construction and gene mapping in *Candida albicans*. Genetics **134:**717–728.
33. **Fortwendel, J. R., et al.** 2009. Differential effects of inhibiting chitin and 1,3-β-D-glucan synthesis in ras and calcineurin mutants of *Aspergillus fumigatus*. Antimicrob. Agents Chemother. **53:**476–482.
34. **Gasparoto, T. H., et al.** 2009. Isolation of *Candida dubliniensis* from denture wearers. J. Med. Microbiol. **58:**959–962.
35. **Gilfillan, G. D., et al.** 1998. *Candida dubliniensis*: phylogeny and putative virulence factors. Microbiology **144:**829–838.
36. **Gillum, A. M., E. Y. Tsay, and D. R. Kirsch.** 1984. Isolation of the *Candida albicans* gene for orotidine-5′-phosphate decarboxylase by complementation of *S. cerevisiae ura3* and *E. coli pyrF* mutations. Mol. Gen. Genet. **198:**179–182.
37. **Greenblatt, M. B., A. Aliprantis, B. Hu, and L. H. Glimcher.** 2010. Calcineurin regulates innate antifungal immunity in neutrophils. J. Exp. Med. **207:** 923–931.
38. **Hemady, R. K.** 1995. Microbial keratitis in patients infected with the human immunodeficiency virus. Ophthalmology **102:**1026–1030.
39. **Hemady, R. K., N. Griffin, and B. Aristimuno.** 1993. Recurrent corneal infections in a patient with the acquired immunodeficiency syndrome. Cornea **12:**266–269.
40. **Jabra-Rizk, M. A., et al.** 2005. Prevalence of *Candida dubliniensis* fungemia at a large teaching hospital. Clin. Infect. Dis. **41:**1064–1067.
41. **Jackson, A. P., et al.** 2009. Comparative genomics of the fungal pathogens *Candida dubliniensis* and *Candida albicans*. Genome Res. **19:**2231–2244.
42. **Karababa, M., et al.** 2006. *CRZ1*, a target of the calcineurin pathway in *Candida albicans*. Mol. Microbiol. **59:**1429–1451.
43. **Kofteridis, D. P., R. E. Lewis, and D. P. Kontoyiannis.** 2010. Caspofungin-non-susceptible *Candida* isolates in cancer patients. J. Antimicrob. Chemother. **65:**293–295.
44. **Kojima, K., Y. S. Bahn, and J. Heitman.** 2006. Calcineurin, Mpk1 and Hog1 MAPK pathways independently control fludioxonil antifungal sensitivity in *Cryptococcus neoformans*. Microbiology **152:**591–604.
45. **Kontoyiannis, D. P., et al.** 2008. Calcineurin inhibitor agents interact synergistically with antifungal agents in vitro against *Cryptococcus neoformans* isolates: correlation with outcome in solid organ transplant recipients with cryptococcosis. Antimicrob. Agents Chemother. **52:**735–738.
46. **LaFayette, S. L., et al.** 2010. PKC signaling regulates drug resistance of the fungal pathogen *Candida albicans* via circuitry comprised of Mkc1, calcineurin, and Hsp90. PLoS Pathog. **6:**e1001069.
47. **Lo, H. J., et al.** 1997. Nonfilamentous *C. albicans* mutants are avirulent. Cell **90:**939–949.
48. **Marcos-Arias, C., et al.** 2009. Isolation of *Candida dubliniensis* in denture stomatitis. Arch. Oral Biol. **54:**127–131.
49. **McManus, B. A., et al.** 2009. Genetic differences between avian and human isolates of *Candida dubliniensis.* Emerg. Infect. Dis. **15:**1467–1470.
50. **Miyazaki, T., et al.** 2010. Roles of calcineurin and Crz1 in antifungal susceptibility and virulence of *Candida glabrata*. Antimicrob. Agents Chemother. **54:**1639–1643.

51. **Monge, R. A., E. Roman, C. Nombela, and J. Pla.** 2006. The MAP kinase signal transduction network in *Candida albicans*. Microbiology **152:**905–912.
52. **Moran, G. P., et al.** 1997. Antifungal drug susceptibilities of oral *Candida dubliniensis* isolates from human immunodeficiency virus (HIV)-infected and non-HIV-infected subjects and generation of stable fluconazole-resistant derivatives in vitro. Antimicrob. Agents Chemother. **41:**617–623.
53. **Mylonakis, E., et al.** 2005. *Galleria mellonella* as a model system to study *Cryptococcus neoformans* pathogenesis. Infect. Immun. **73:**3842–3850.
54. **Nett, J. E., K. Marchillo, C. A. Spiegel, and D. R. Andes.** 2010. Development and validation of an in vivo *Candida albicans* biofilm denture model. Infect. Immun. **78:**3650–3659.
55. **Noble, S. M., S. French, L. A. Kohn, V. Chen, and A. D. Johnson.** 2010. Systematic screens of a *Candida albicans* homozygous deletion library decouple morphogenetic switching and pathogenicity. Nat. Genet. **42:**590–598.
56. **Nunn, M. A., S. M. Schaefer, M. A. Petrou, and J. R. Brown.** 2007. Environmental source of *Candida dubliniensis.* Emerg. Infect. Dis. **13:**747–750.
57. **O'Connor, L., N. Caplice, D. C. Coleman, D. J. Sullivan, and G. P. Moran.** 2010. Differential filamentation of *Candida albicans* and *C. dubliniensis* is governed by nutrient regulation of *UME6* expression. Eukaryot. Cell **9:**1383–1397.
58. **Odds, F. C., A. J. Brown, and N. A. Gow.** 2003. Antifungal agents: mechanisms of action. Trends Microbiol. **11:**272–279.
59. **Odom, A., et al.** 1997. Calcineurin is required for virulence of *Cryptococcus neoformans*. EMBO J. **16:**2576–2589.
60. **Onyewu, C., N. A. Afshari, and J. Heitman.** 2006. Calcineurin promotes infection of the cornea by *Candida albicans* and can be targeted to enhance fluconazole therapy. Antimicrob. Agents Chemother. **50:**3963–3965.
61. **Onyewu, C., J. R. Blankenship, M. Del Poeta, and J. Heitman.** 2003. Ergosterol biosynthesis inhibitors become fungicidal when combined with calcineurin inhibitors against *Candida albicans*, *Candida glabrata*, and *Candida krusei*. Antimicrob. Agents Chemother. **47:**956–964.
62. **Onyewu, C., F. L. Wormley, Jr., J. R. Perfect, and J. Heitman.** 2004. The calcineurin target, Crz1, functions in azole tolerance but is not required for virulence of *Candida albicans*. Infect. Immun. **72:**7330–7333.
63. **Park, H., et al.** 2005. Role of the fungal Ras-protein kinase A pathway in governing epithelial cell interactions during oropharyngeal candidiasis. Cell. Microbiol. **7:**499–510.
64. **Perea, S., et al.** 2002. Molecular mechanisms of fluconazole resistance in *Candida dubliniensis* isolates from human immunodeficiency virus-infected patients with oropharyngeal candidiasis. Antimicrob. Agents Chemother. **46:**1695–1703.
65. **Perfect, J. R., N. Ketabchi, G. M. Cox, C. W. Ingram, and C. L. Beiser.** 1993. Karyotyping of *Cryptococcus neoformans* as an epidemiological tool. J. Clin. Microbiol. **31:**3305–3309.
66. **Reuss, O., A. Vik, R. Kolter, and J. Morschhauser.** 2004. The *SAT1* flipper, an optimized tool for gene disruption in *Candida albicans*. Gene **341:**119–127.
67. **Roncero, C., and A. Duran.** 1985. Effect of calcofluor white and congo red on fungal cell wall morphogenesis: in vivo activation of chitin polymerization. J. Bacteriol. **163:**1180–1185.
68. **Sanglard, D., F. Ischer, O. Marchetti, J. Entenza, and J. Bille.** 2003. Calcineurin A of *Candida albicans*: involvement in antifungal tolerance, cell morphogenesis and virulence. Mol. Microbiol. **48:**959–976.
69. **Santos, M., and I. F. de Larrinoa.** 2005. Functional characterization of the *Candida albicans CRZ1* gene encoding a calcineurin-regulated transcription factor. Curr. Genet. **48:**88–100.
70. **Singh, S. D., et al.** 2009. Hsp90 governs echinocandin resistance in the pathogenic yeast *Candida albicans* via calcineurin. PLoS Pathog. **5:**e1000532.
71. **Spiering, M. J., et al.** 2010. Comparative transcript profiling of *Candida albicans* and *Candida dubliniensis* identifies *SFL2*, a *C. albicans* gene required for virulence in a reconstituted epithelial infection model. Eukaryot. Cell **9:**251–265.
72. **Stathopoulos, A. M., and M. S. Cyert.** 1997. Calcineurin acts through the *CRZ1*/*TCN1*-encoded transcription factor to regulate gene expression in yeast. Genes Dev. **11:**3432–3444.
73. **Steinbach, W. J., et al.** 2006. Calcineurin controls growth, morphology, and pathogenicity in *Aspergillus fumigatus*. Eukaryot. Cell **5:**1091–1103.
74. **Steinbach, W. J., et al.** 2007. Calcineurin inhibition or mutation enhances cell wall inhibitors against *Aspergillus fumigatus*. Antimicrob. Agents Chemother. **51:**2979–2981.
75. **Steinbach, W. J., J. L. Reedy, R. A. Cramer, Jr., J. R. Perfect, and J. Heitman.** 2007. Harnessing calcineurin as a novel anti-infective agent against invasive fungal infections. Nat. Rev. Microbiol. **5:**418–430.
76. **Stie, J., and D. Fox.** 2008. Calcineurin regulation in fungi and beyond. Eukaryot. Cell **7:**177–186.
77. **Stokes, C., et al.** 2007. Lower filamentation rates of *Candida dubliniensis* contribute to its lower virulence in comparison with *Candida albicans*. Fungal Genet. Biol. **44:**920–931.
78. **Sullivan, D. J., G. P. Moran, and D. C. Coleman.** 2005. *Candida dubliniensis*: ten years on. FEMS Microbiol. Lett. **253:**9–17.
79. **Sullivan, D. J., et al.** 2004. Comparison of the epidemiology, drug resistance mechanisms, and virulence of *Candida dubliniensis* and *Candida albicans*. FEMS Yeast Res. **4:**369–376.
80. **Sullivan, D. J., T. J. Westerneng, K. A. Haynes, D. E. Bennett, and D. C. Coleman.** 1995. *Candida dubliniensis* sp. nov.: phenotypic and molecular characterization of a novel species associated with oral candidosis in HIV-infected individuals. Microbiology **141:**1507–1521.
81. **Tappeiner, C., D. Goldblum, S. Zimmerli, C. Fux, and B. E. Frueh.** 2009. Donor-to-host transmission of *Candida glabrata* to both recipients of corneal transplants from the same donor. Cornea **28:**228–230.
82. **Thompson, G. R., III, et al.** 2010. Oropharyngeal candidiasis in the era of antiretroviral therapy. Oral Surg. Oral Med. Oral Pathol. Oral Radiol. Endod. **109:**488–495.
83. **Tukmachev, V. A., L. V. Nedospasova, B. Zaslavskii, and S. V. Rogozhin.** 1979. Effect of sodium dodecyl sulfate on biological membranes. Biofizika **24:**55–60. (In Russian.)
84. **Uppuluri, P., J. Nett, J. Heitman, and D. Andes.** 2008. Synergistic effect of calcineurin inhibitors and fluconazole against *Candida albicans* biofilms. Antimicrob. Agents Chemother. **52:**1127–1132.
85. **Vilela, M. M., et al.** 2002. Pathogenicity and virulence of *Candida dubliniensis*: comparison with *C. albicans*. Med. Mycol. **40:**249–257.
86. **Walker, L. A., N. A. Gow, and C. A. Munro.** 2010. Fungal echinocandin resistance. Fungal Genet. Biol. **47:**117–126.
87. **Walker, L. A., et al.** 2008. Stimulation of chitin synthesis rescues *Candida albicans* from echinocandins. PLoS Pathog. **4:**e1000040.
88. **Watts, H. J., A. A. Very, T. H. Perera, J. M. Davies, and N. A. Gow.** 1998. Thigmotropism and stretch-activated channels in the pathogenic fungus *Candida albicans*. Microbiology **144:**689–695.
89. **Wu, T. G., K. R. Wilhelmus, and B. M. Mitchell.** 2003. Experimental keratomycosis in a mouse model. Invest. Ophthalmol. Vis. Sci. **44:**210–216.
90. **Yadan, J. C., M. Gonneau, P. Sarthou, and F. Le Goffic.** 1984. Sensitivity to nikkomycin Z in *Candida albicans*: role of peptide permeases. J. Bacteriol. **160:**884–888.
91. **Yoshida, T., T. Toda, and M. Yanagida.** 1994. A calcineurin-like gene *ppb1* in fission yeast: mutant defects in cytokinesis, cell polarity, mating and spindle pole body positioning. J. Cell Sci. **107:**1725–1735.